Mineral Provinces

17

Fluid inclusion and oxygen isotope data and summary of evidence for low-temperature gold, platinum and palladium (±uranium) mineralisation at Coronation Hill, Northern Territory, Australia. Record 1992/69.

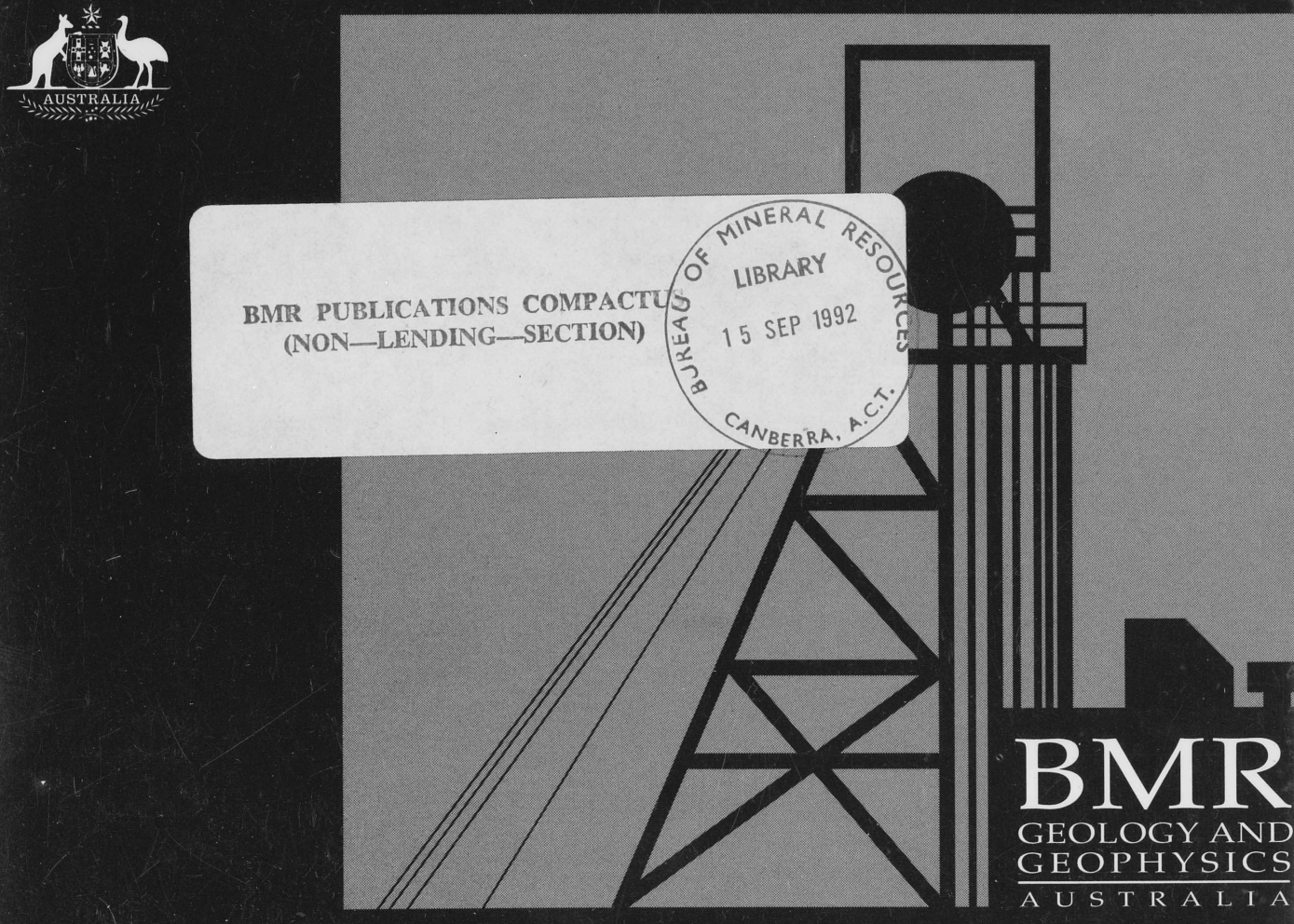

BMR
GEOLOGY AND GEOPHYSICS
AUSTRALIA

T P Mernagh[1], J F Leckie[2] and D P Carville[3]

MINERALS AND LAND USE PROGRAM
BUREAU OF MINERAL RESOURCES, GEOLOGY AND GEOPHYSICS

BMR
GEOLOGY AND
GEOPHYSICS
AUSTRALIA

Fluid inclusion and oxygen isotope data and summary of evidence for low-temperature gold, platinum and palladium (±uranium) mineralisation at Coronation Hill, Northern Territory, Australia. Record 1992/69.

T P Mernagh[1], J F Leckie[2] and D P Carville[3]

[1] Bureau of Mineral Resources, GPO Box 378 Canberra ACT 2601 Australia
[2] Newcrest Mining Ltd, PO Box 1367 Milton Qld 4064 Australia
[3] Newcrest Mining Ltd, PO Box 211, Cloverdale WA 6015 Australia

DEPARTMENT OF PRIMARY INDUSTRIES AND ENERGY

Minister for Resources: The Hon. Alan Griffiths
Secretary: G.L. Miller

BUREAU OF MINERAL RESOURCES, GEOLOGY AND GEOPHYSICS
Executive Director: R.W.R. Rutland AO

ISSN 0811 062X
ISBN 0 642 18406 2

TABLE OF CONTENTS

SUMMARY

Coronation Hill, Northern Territory, Australia, is a low-temperature, hydrothermal Au-Pt-Pd prospect containing restricted zones of uranium. All mineralisation is confined to stratigraphic units below a lower Proterozoic unconformity which separates the deformed and metamorphosed sequence of igneous intrusives, volcaniclastics and carbonaceous units from the little-deformed, overlying, hematitic quartz sandstone. Two styles of unconformity-related mineralisation have been recognised. The main Au-platinum group elements (PGE) ore is widely distributed and occurs in several stratigraphic units while minor U-Au-PGE mineralisation has also been observed in a number of stratigraphic units and intrusives.

The hydrothermal transport of Au, Pt, Pd and U in mineralising fluids at Coronation Hill was investigated by studying fluid inclusions in both mineralised and unmineralised quartz and carbonate veins. The inclusions generally have irregular shapes and show evidence of necking. Four types have been recognized; (i) vapour-rich inclusions; (ii) two phase aqueous inclusions containing approximately 5 vol. % vapour; (iii) single phase, liquid inclusions and (iv) rare inclusions containing up to four solid phases and 10 vol. % vapour. Many microfractures contain only vapour-rich inclusions indicating that a separate vapour phase was present at some stage. The single phase liquid inclusions coexist with the vapour-rich inclusions and probably resulted from the process of necking down. The inclusions containing solid phases represent early regional fluids while the other inclusions are thought to result from the ore-forming fluid.

Microthermometry indicates that the ore fluids were saline and calcium-dominated (ca. 30 equiv. wt % $CaCl_2$) and that mineralisation occurred at around 140°C. The high calcium content of the fluids was verified by low temperature Raman spectroscopy. Generally, no gases were detected in the vapour phase. However, O_2 was detected in inclusions close to pitchblende mineralisation indicating that radiolysis may have occurred. Solid inclusions of calcite, hematite and white mica in the Type C inclusions were detected by Raman spectroscopy.

The fluid inclusion data indicate that U, Au and PGE were all transported in the same highly oxidised, low pH and calcium rich brine. At these conditions transport of Au and PGE would involve mainly chloride complexes while uranium could be transported as either uranium oxy or oxy-chloride species. Isotopic evidence suggests that the ore fluids were originally saline groundwaters which travelled downwards in the mineralised zone. The precipitation of Au-PGE only ore is thought to result from fluid-rock interactions which lead to a moderate reduction in log fO_2 and an increase in solution pH to K-feldspar buffered values around pH 5. U-Au-PGE mineralisation is mainly associated with structural shear zones and possibly results from the mixing of the oxidised fluid with a reduced fluid originating from the carbonaceous units below the unconformity.

INTRODUCTION

This fluid inclusion study was undertaken as part of a collaborative study of the Coronation Hill prospect by the Bureau of Mineral Resources and the partners in the Coronation Hill Joint Venture (CHJV). The data presented in this Record is in support of a paper entitled "*Chemistry of low-temperature hydrothermal gold, platinum and palladium (±uranium) mineralization at Coronation Hill, Northern Territory, Australia*" to be published in the Economic Geology journal. This paper will also contain detailed discussions of the data and the proposed mineralisation mechanisms.

There is increasing evidence that hydrothermal fluids play an important role in the transport of Au and PGE in a variety of environments. Hydrothermal PGE mineralisation has been reported from many deposits associated with layered mafic-ultramafic intrusives (e.g. Stumpfl, 1974; Mathez, 1989) but the hydrothermal activity may not always be linked to mafic magmatism (e.g. Hewett, 1956; Mihalik, *et al.*, 1974). In fact, many workers have proposed that the PGE are mobilised during or after the formation of such magmatic PGE deposits (e.g. Volborth and Housley, 1984; Ballhaus and Stumpfl, 1986; Dillon-Leitch *et al.*, 1986; Nyman *et al.*, 1990). Studies of the mobilisation of PGE in the supergene zone (Ottemann and Augustithis, 1967; Fuchs and Rose, 1974; Plimer and Williams, 1988) have indicated that PGE can be transported in relatively low temperature fluids, and recently, Watkinson and Melling (1992) have reported that the Cu-Au-Pd-Ag deposit in the Salt Chuck intrusion, Alaska was formed from a low temperature, saline, calcium bearing hydrothermal fluid.

Hydrothermal Au and PGE are also found in significant concentrations in the unconformity-related uranium deposits of the South Alligator Valley Mineral Field and the Alligator Rivers Uranium Field in the Northern Territory, Australia (Needham, 1987). For example, mines in the South Alligator Valley Mineral Field have collectively produced 70,000g of Au (Foy, 1975) and the Jabiluka deposit contains Au at an average grade of 10 g/tonne and significant but subeconomic concentrations of Pd (Wilde *et al.*, 1989a). It is also worth noting that a few of the unconformity-related deposits in the Athabasca basin in Canada have also been reported to contain minor concentrations of Au and PGE (Wray *et al.*, 1985).

The Coronation Hill Au-Pt-Pd deposit is located in the upper part of the South Alligator River Valley at latitude 13°35'S and longitude 132°36'E, and is approximately 80 km east of the town of Pine Creek in the Northern Territory, Australia. This area was the scene of uranium mining in the 1950s and 1960s and during this period thirteen small uranium mines were in operation and some forty-six prospects were explored. At this time, 25,306 tonnes of uranium ore grading 0.26% U_3O_8 containing 33,600 kg U_3O_8 were produced by open cut and underground mining (Fisher, 1969). Gold mineralisation was concomitant with uranium mineralisation and gold was produced by gravity separation and later by cyanide extraction from uranium ore.

The Coronation Hill Joint Venture which currently consists of Newcrest Mining Ltd. (45%), Plutonic Resources Ltd. (45%) and Norgold Ltd. (10%) commenced exploration specifically for gold in the Coronation Hill area in 1984 and following initially encouraging results, exploration continued through to mid 1988. The results of this investigation gave an indicated resource of 3.49 million tonnes at 5.12 g/t Au, 0.21 g/t Pt and 0.56 g/t Pd with a further inferred resource of 2.87 million tonnes at 7.25 g/t Au, 0.35 g/t Pt and 1.31 g/t Pd.

REGIONAL GEOLOGICAL SETTING

Two of Australia's important uranium mineral provinces; the Alligator Rivers Uranium Field and the South Alligator Valley Mineral Field lie in the eastern trough of the Pine Creek Geosyncline. This region has an Archean and lower Proterozoic basement of regionally deformed metasediments and felsic meta-igneous rocks which are intruded by granites and dolerite. The basement is unconformably overlain by the Katherine River Group which comprises the hematitic alluvial sandstone of the Kombolgie Formation and interbedded mafic volcanic rocks (Needham *et al.*, 1980).

The tectonic evolution of the Pine Creek Geosyncline has been described (Needham *et al.*, 1988) as a main rift sequence of pre-1880 Ma rift, sag and orogenic phases of sedimentation and igneous activity, which are overprinted by the "Nimbuwah Event" , a phase of low to moderate pressure metamorphism and crustal shortening involving tectonic transport from northeast to southwest. The South Alligator Valley straddles the boundary between greenschist and amphibolite facies metamorphism in the main rift sequence (Warren and Kamprad, 1990). Needham *et al.*, (1988) described two later "episodes" of rifting separated by "episodes" of crustal shortening, implying alternating shortening and extension about northeast-southwest axes on faults parallel to the northwest trending structural grain of the pre-Nimbuwah basement. The El Sherana Group and Edith River Group "rift fill" sequences show sediment transport parallel to northwest-trending faults (Needham *et al.*, 1988). The South Alligator Valley occurs within a zone of complex and long-lived reactivation of the basement structural grain, producing spatially and temporally coexisting zones of shortening about northeast trending axes and the pattern of late faults in the South Alligator Valley is consistent with dextral strike slip displacement on northwest-trending faults.

The mineral deposits of the Alligator Rivers Uranium Field are located within and adjacent to reverse fault zones of minor displacement. An outer zone of alteration extends over 1 km from the ore which is also associated with a more restricted inner zone of alteration in the basement, and along and above the sub-Kombolgie unconformity (Gustafson and Curtis, 1983; Wilde and Wall, 1987; Wilde *et al.*, 1989b). Intense desilification has been observed around the orebodies (Wilde and Wall, 1987) and most premineralisation phases were removed during alteration. Mineralisation occurs close to and often within, graphitic horizons in the lower Proterozoic sequence and very little of the ore is hosted by the Kombolgie Formation. However, many of the orebodies (e.g. Nabarlek, Koongarra and Jabiluka) have had their Kombologie Formation cover removed by erosion.

Most of the mineralisation in the South Alligator Valley is contained within the major northwest trending Rockhole-El Sherana-Palette fault system. All known deposits are surrounded by alteration zones that may extend for over one kilometre. The alteration is characterised mineralogically by sericite/ chlorite ± kaolinite ± biotite ± hematite with hematite being the most extensive type of alteration. At some of the deposits (e.g. El Sherana) the rocks are strongly desilicified at the sub-Kombolgie unconformity and consist of predominantly chlorite-rich felsic volcanics which still retain some primary volcanic textures such as flow-banding and quartz phenocrysts. In other places, generally at higher stratigraphic levels (e.g. Coronation Hill) the volcanics are silicified and quartz-veined.

Although there are similarities between the deposits in the South Alligator Valley and the

Alligator Rivers Uranium Field there are also several important differences. In the Alligator Rivers Uranium Field the host rocks below the unconformity are the carbonate and carbonaceous schists of the lower Cahill Formation and its presumed lateral equivalent, the Myra Falls Metamorphics, whereas, in the South Alligator Valley it is the Koolpin Formation which mainly consists of carbonaceous pelitic sediments and dolomite. Geochronological dating indicates that the mineralisation may be as young as 600-900 Ma (Greenhalgh and Jeffrey, 1959).

GEOLOGICAL SETTING OF CORONATION HILL

The geology of the Coronation Hill deposit has been described in detail by Carville *et al.,* (1990 and 1991). An interpretation of the local stratigraphy and its correlation with the regional stratigraphy has also been given in Carville *et al.*, (1991). The oldest rocks recognised at Coronation Hill are those of the Koolpin Formation which outcrop to the east of the Palette Fault as intensely contact metamorphosed and finely interbedded ferruginous slates and quartzites. Stromatolitic dolomite, often recrystallised, was also intersected in deep diamond drill-holes at Coronation Hill and is correlated with stromatolitic bioherms of the Koolpin Formation which outcrop approximately 2.5 km to the north-west. A dark green siltstone outcrops to the south of the mineralised zone and is upfaulted and is interpreted to be part of the Koolpin Formation.

Overlying the Koolpin Formation is a unit of predominantly green chlorite-altered volcaniclastic sediments interbedded with minor shale and chert. These volcaniclastics are believed to be the equivalent of the Shovel Billabong Andesite. This unit is unconformably overlain by a sedimentary breccia, referred to informally as Type C breccia. A grey quartz arenite is associated with the breccia which contains predominantly clasts of amygdaloidal basalt, but clasts of chlorite altered volcaniclastics, altered quartz feldspar porphyry and medium grained basic intrusives also occur. The breccia postdates the hydrothermal alteration of the volcaniclastic sediments, the quartz feldspar intrusives and the medium grained basic intrusive (see below).

Two suites of intrusive rocks, quartz feldspar porphyries and medium grained basic intrusives, are known from outcrop and drill core at Coronation Hill. The quartz feldspar intrusives are rhyolitic in composition and are essentially identical although one predates, and one postdates the basic intrusive. The earlier quartz feldspar porphyry exhibits flow banding and is xenolith free, while the later porphyry contains xenoliths of the basic intrusives and the green siltstone. The centre of intrusion of the porphyries appears to be approximately 1 km to the southeast of Coronation Hill and the porphyries have been correlated with dacite which intrudes the Gerowie Tuff some 43 km to the northwest. The basic intrusives consist predominantly of medium to coarse grained micrographic quartz diorite, but adamellite, granodiorite, monzodiorite, dolerite and diorite have also been observed. They are of hypabyssal to plutonic origin and can be correlated with intrusives of the Zamu Dolerite (Warren and Kamprad, 1990). Fragments of both the porphyries and the quartz diorite occur in the Type C breccia thus indicating that the intrusives are older than the unconformity at the base of this breccia.

Unconformably overlying the igneous intrusives and the Type C breccia is a prominent hematitic, quartz sandstone unit known as the capping sandstone. The base of the sandstone is marked by a conglomerate of pebbles and cobbles of quartz sandstone and white vein quartz. The capping sandstone is considered to be the base of the Kombolgie Formation and the pebble

conglomerate is thought to mark the sub-Kombolgie unconformity. In faulted contact with the lithologies below this unconformity is a unit of debris flow conglomerate described by Needham and Stuart-Smith (1987) and has been subdivided into Types A and B by Carville *et al.*, (1990). The sedimentary breccias postdate the capping sandstone as indicated by the sandstone and white quartz clasts found in the Type A breccia.

Structure

The major structure at Coronation Hill is an east-west trending, south dipping reverse fault which has brought the quartz feldspar porphyry, volcaniclastic sediments, quartz diorite and Type A and B breccias into a position overlying the Type C breccia and carbonaceous units of the Koolpin Formation (see Figure 1). An east-west trending and possibly reverse fault to the south brings green siltstone of the Koolpin formation into contact with the mineralised sequence.

Mineralisation occurs on a set of parallel, north-northwest trending, sub-vertical faults, down throwing to the west and almost parallel to the regional Palette Fault. It appears to have occurred during or after fault movement, as indicated by the fact that it occurs in lithologies of various ages in association with the north-northwest trending fault zone. There is also evidence for east-northeast faulting, postdating mineralisation, which may dislocate the major structurally controlled ore zones slightly to the west, causing the ore shoots to be discontinuous.

Alteration

Early chloritic alteration has been observed in the volcaniclastics which are universally altered to a chlorite-sericite-quartz-sphene assemblage. The quartz diorite was similarly altered to a quartz-chlorite-sericite assemblage with minor sphene, leucoxene and pyrite. Alteration of the quartz feldspar porphyry is characterised by a quartz-sericite assemblage with trace amounts of pyrite, chlorite, carbonate, dumortierite and sphene. Quartz and carbonate veining is common and some pervasive silicification has been observed. This phase of alteration is associated with the development of ductile foliations which are known to predate the El Sherana Group (Wyborn *et al.*, 1991).

A pervasive hematitic alteration event followed and involved the introduction of fine grained earthy hematite into all lithologies below the Type C breccia and caused primary textures to be obliterated in the most intense zones. Pyrite was oxidized to hematite except in zones of pervasive silicification. Porphyry clasts in the Type C breccia have been subjected to this phase of alteration before deposition indicating that it occurred during the erosion event marked by the unconformity at the base of the breccia. This phase of alteration predates mineralisation as it is clearly replaced by chloritic alteration envelopes which occur in association with some of the mineralised veins, especially those associated with high grade uranium mineralisation. Although the mineralisation is confined to the alteration assemblages there is no correlation with the intensity of the alteration.

Finally, all lithologies including the capping sandstone are generally overprinted by a later, fracture-related event which involved the introduction of earthy hematite and specular hematite along fractures. In addition to these alteration types observed by Carville *et al.*, (1990, 1991), Warren and Kamprad (1990) have also identified a regional scale carbonate alteration which is evident in parts of Coronation Hill.

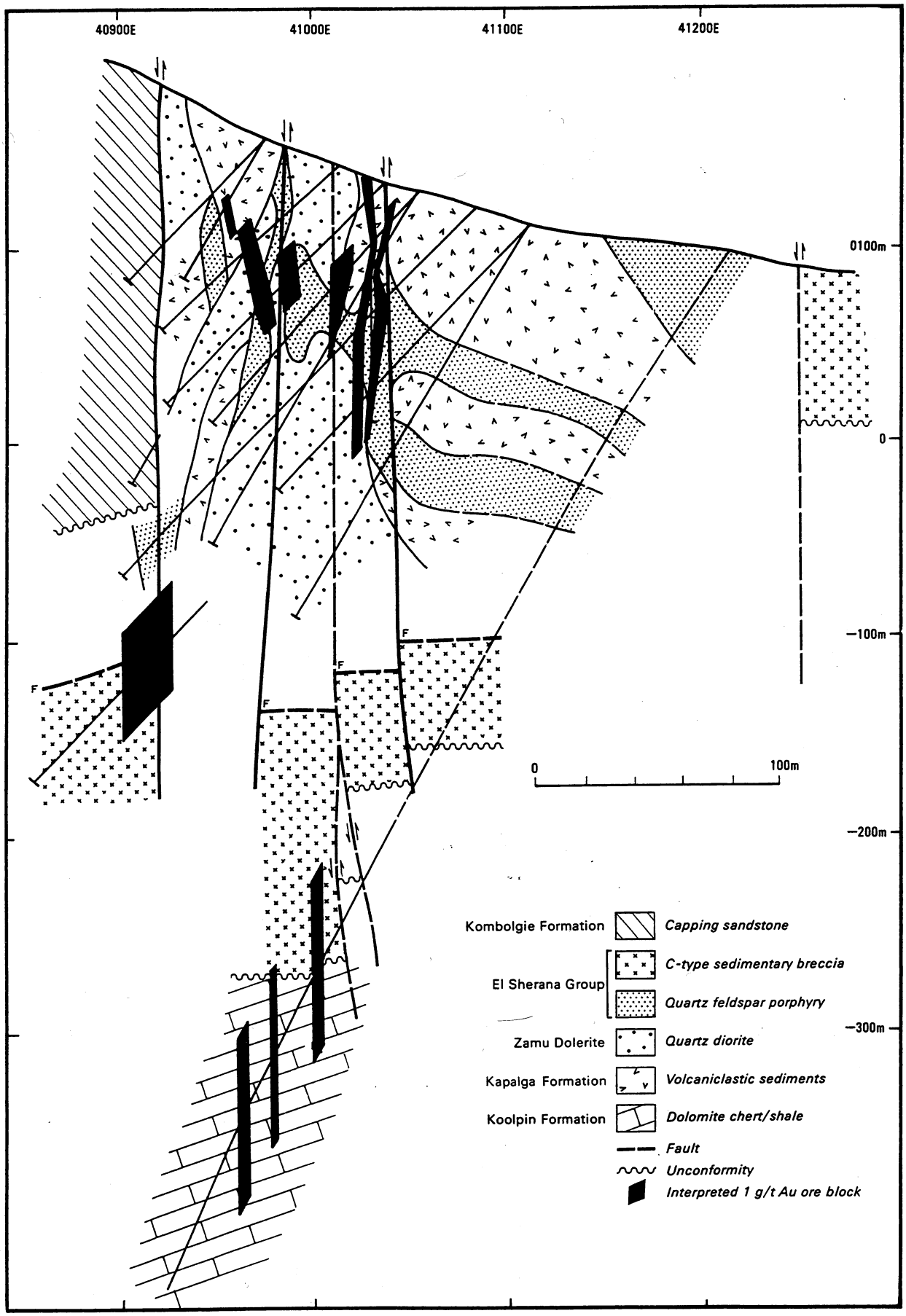

Figure 1. Interpretative geological cross section of the Coronation Hill prospect.

Mineralisation

Gold, Pt, Pd, and sometimes U minerals occur in microfractures in quartz/carbonate/hematite veinlets and as disseminated mineralisation within the sericitic-chloritic alteration matrix in the altered igneous host rocks where it is often closely associated with replacive pyrite. Graphite or carbonaceous material of suspected hydrothermal origin occurs in some veinlets and within the alteration matrix. Veinlet paragenesis is complex but mineralised veins are generally undeformed, suggesting a late timing for mineralisation.

The mineralisation can be broadly separated into two types. The first is U-Au-PGE ore found at or below the sub-Kombolgie unconformity. This style of mineralisation occurs rarely in a subvertical zone and is generally restricted to conglomerates containing carbonaceous clasts and also to chloritic zones, which alter the quartz feldspar porphyry. Visible and disseminated gold occurs with the uranium which consists of disseminated and patchy pitchblende with minor secondary uranium minerals occurring at the surface (Needham, 1987).

The second type is Au-PGE ore with a very low uranium content which occurs in irregular quartz-carbonate-chlorite veins or breccias in the quartz-feldspar porphyry, the quartz diorite and the volcaniclastics. This ore type is confined to the stratigraphic units below sub-Kombolgie unconformity but otherwise appears to have no lithological control (c.f. Figure 1). Two distinct mineralogical associations of Au-PGE ore have been recognized (Gilbert, 1987):

- (i) A Au-PGE-selenide association comprising Au in both pure and silver bearing varieties, clausthalite (PbSe), stibiopalladinite (Pd_5Sb_2) and native Pd. Platinum is less common but is present as (Pt, Pd) Se_2, $PtSe_2$, a Pt-Pd-Fe alloy and rare native platinum.

- (ii) A Au-PGE-selenide-sulfide association which also contains the minerals listed above together with replacive pyrite, occurring mainly in the altered igneous host rocks.

Gold-PGE mineralisation is not intimately related to the pyrite content and overall the sulfide content is generally low, with minor pyrite and traces of marcasite, pyrrhotite, sphalerite, chalcopyrite and galena. A small zone of copper mineralisation also occurs in the quartz breccias close to the surface. Some copper mineralisation is to be expected as it is often a major component of other similar hydrothermal Cu-Au-PGE deposits (Kucha, 1982; Nyman *et al.*, 1990; Watkinson and Melling, 1992).

NATURE AND OCCURRENCE OF FLUID INCLUSIONS

Fluid inclusions were examined in 50 thin sections from 62 samples of diamond drill core containing either quartz or carbonate veining. Highly mineralised veins were selected from the assay data and fluid inclusions intimately associated with the mineralisation could be readily observed. Note that previous studies of Australian unconformity-related deposits have not been able to provide direct evidence of a link between the fluid inclusions and mineralisation (e.g. Ypma and Fuzikawa, 1980; Wilde *et al.*, 1989b). Some unmineralised veins and also quartz phenocrysts from the quartz feldspar porphyry were also examined to check for any differences. However, the mineralised and barren veins both contained large numbers of fluid inclusions typically less than 10 μm but occasionally up to 30 μm in diameter.

Sometimes primary inclusions were evident in growth zones within the quartz or carbonate

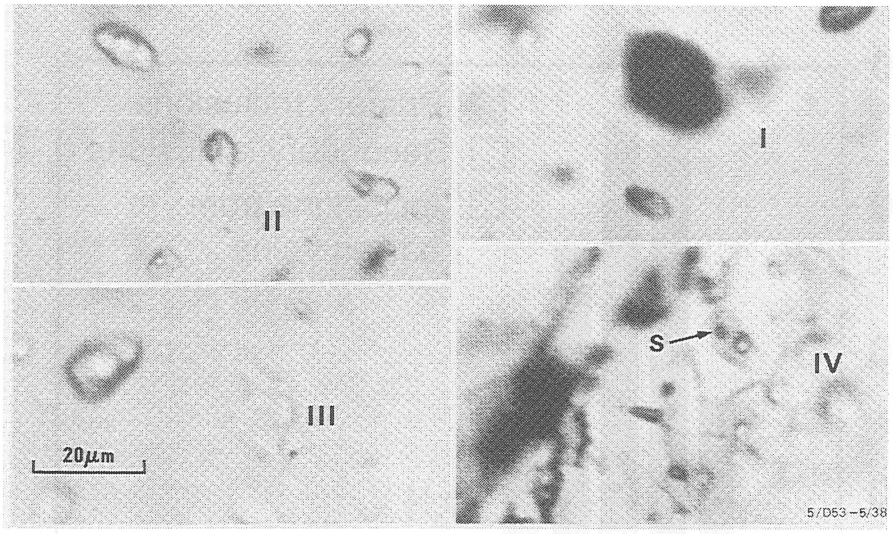

Figure 2. Photomicrographs showing the nature of fluid inclusions from Coronation Hill. The different types of fluid inclusions are denoted as follows: I Type A vapour-rich; II Type B liquid-rich; III Type D monophase aqueous; and IV Type C secondary inclusion with a daughter mineral (S). Scale bar = 20 μm.

crystals. Most of the inclusions, however, occurred as secondary trails along healed fractures which have a criss-crossing, wispy texture which often results from metamorphism or deep burial (Bodnar *et al.,* 1985). Four different types of fluid inclusions were observed in both the quartz and carbonate veins (see Figure 2):

- Type A are vapour rich and contain between 25 and 100 volume % vapour. They are by far the most abundant and often are the only inclusions observed in some microfractures. The inclusions are usually irregularly shaped and show evidence of necking. However, in many cases only 100% vapour inclusions were observed in healed microfractures which indicates that a separate vapour phase existed and that boiling had occurred.

- Type B are two phase aqueous inclusions containing approx. 5 volume % vapour. Some show evidence of necking and their shapes vary from irregular, to rounded to negative crystal but consistent liquid/vapour ratios were usually observed within single microfractures.

- Type C are relatively rare and contain between one and four solid phases, an aqueous phase and typically less than 10 volume % vapour. They mostly contain only one daughter crystal which is sometimes observed to be birefringent. Inclusions with several daughter minerals often contain variable quantities of orange hematite which is thought to be an accidental solid inclusion. Type C inclusions usually have consistent liquid/vapour ratios within individual healed microfractures.

- Type D are one-phase liquid inclusions which coexist with vapour-rich inclusions. This indicates that necking-down and healing of inclusions continued at low temperatures (≤100°C) after the vapour phase had nucleated, and that locally inconsistent liquid/vapour ratios observed in Type A inclusions probably resulted from this necking down process.

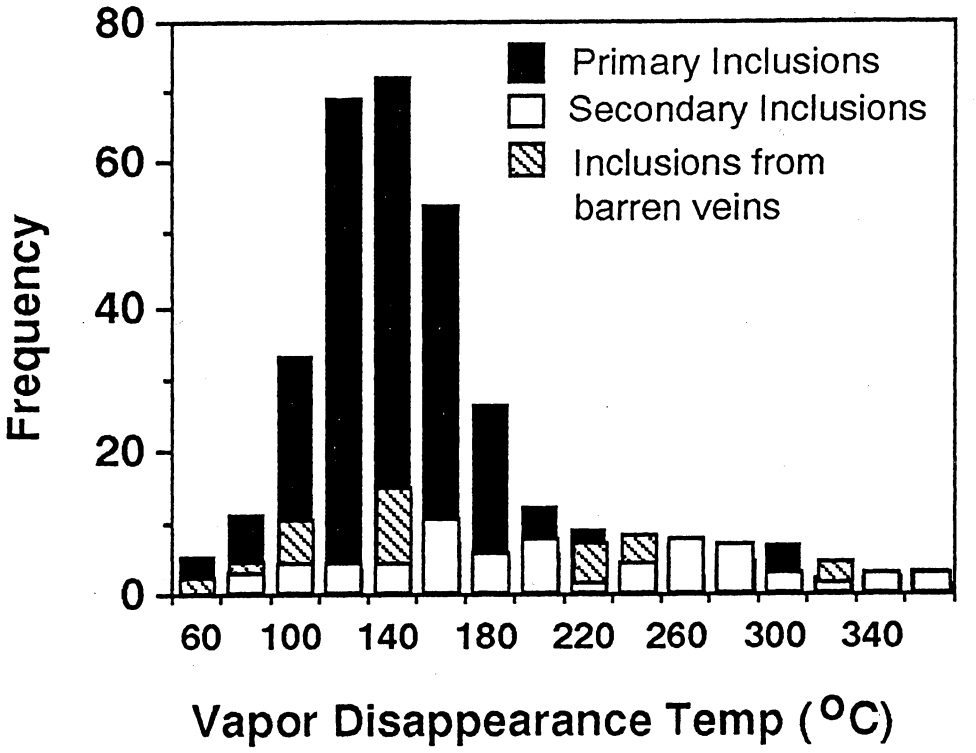

Figure 3. A histogram of vapour disappearance temperatures recorded from microfractures containing inclusions with consistent liquid/vapour ratios. The majority of secondary inclusions occurred in quartz phenocrysts from the quartz feldspar porphyry.

Types A, B and D are primary as they occur together in growth zones in mineralised vein quartz. The two-phase primaries homogenise at approximately 140°C, and the secondaries at around 260°C (see Table 1 and Figure 3). The latter behave similarly to inclusions in samples collected from other parts of the South Alligator River Valley and indicate the passage of regional fluids associated with earlier alteration events.

The freezing behaviour of the fluid inclusions (see Table 1) is complex and was often difficult to observe owing to the small size of most of these inclusions. The primaries exhibit final melting temperatures ranging from -10 to -55°C, but most lie close to the ternary eutectic at -52°C in the H_2O-NaCl-$CaCl_2$ system (see Figure 4). This demonstrates that the fluids have a high $CaCl_2$ content, which was confirmed by recording Raman spectra from frozen fluid inclusions (Figure 5) and data from both methods gave an average salinity of 26.3 equivalent weight percent (wt%) $CaCl_2$ for the primary fluid. The secondary inclusions generally have salinities below 8 equivalent wt% $CaCl_2$, but a small number have intermediate salinities from 10 to 13 equivalent wt% $CaCl_2$, suggesting that some mixing of high and low salinity fluids occurred at a later stage.

The laser Raman microprobe was unable to detect any CO_2, O_2, N_2 or CH_4 in the vapour phase of most of the fluid inclusions. However, O_2 was detected in some zones of high uranium content (Figure 6), but this oxygen is thought to be a product of the radiolysis of the trapped

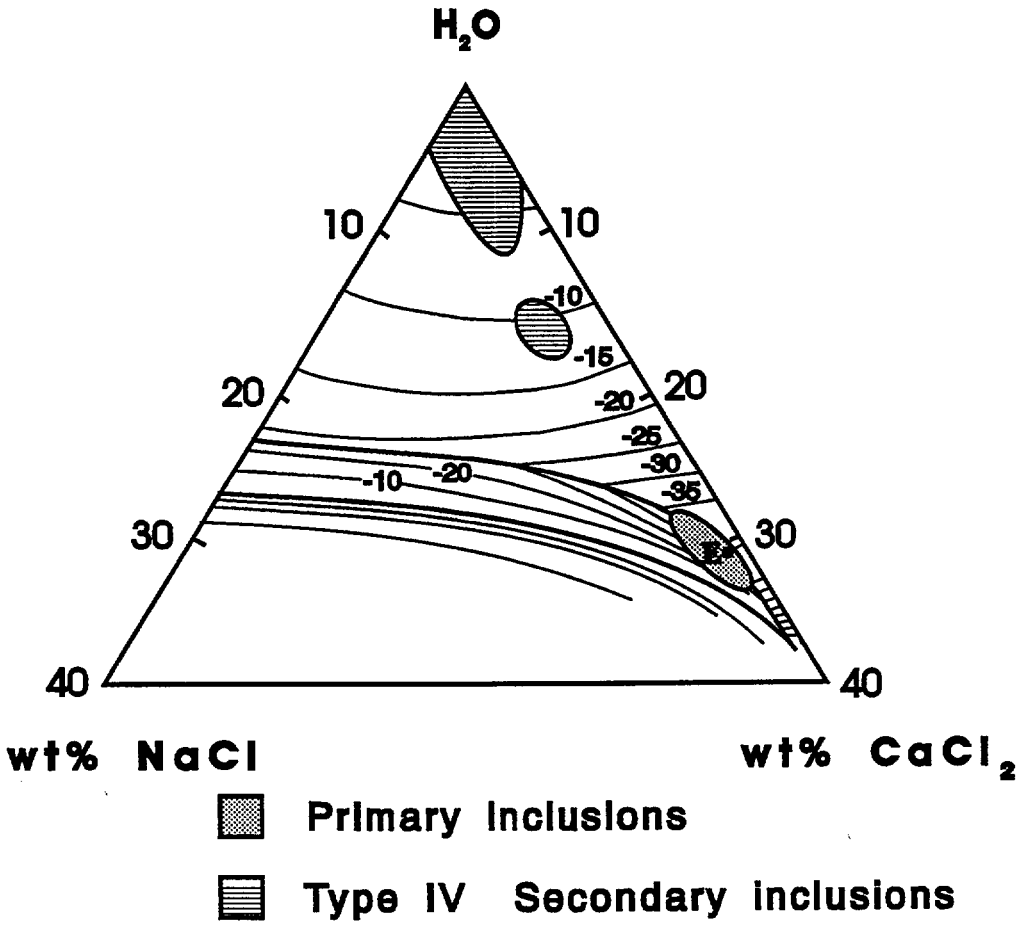

Figure 4. The H_2O-NaCl-$CaCl_2$ ternary system showing the plotted regions for the final melting temperatures of fluids from the primary and secondary inclusions. Point E denotes the ternary eutectic at -52°C.

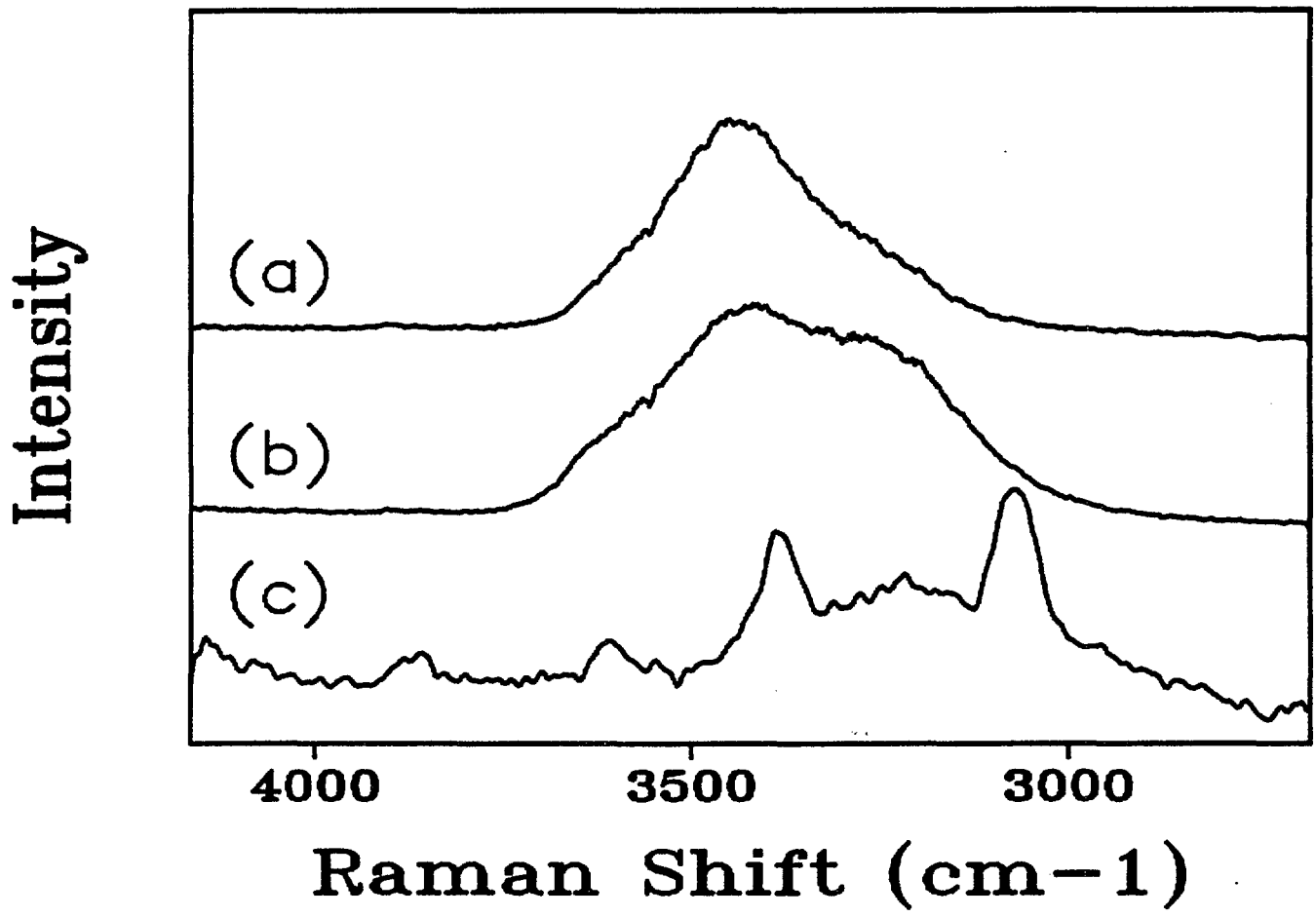

Figure 5. Raman microprobe spectra recorded from (a) the aqueous phase in an inclusion containing 31 equivalent wt% $CaCl_2$, (b) the aqueous phase in an inclusion containing 4 equivalent wt% $CaCl_2$, and (c) the frozen fluid in a primary inclusion at -170°C showing the dominant bands of ice at 3090 cm^{-1} and antarcticite ($CaCl_2.6H_2O$) at 3435 cm^{-1}.

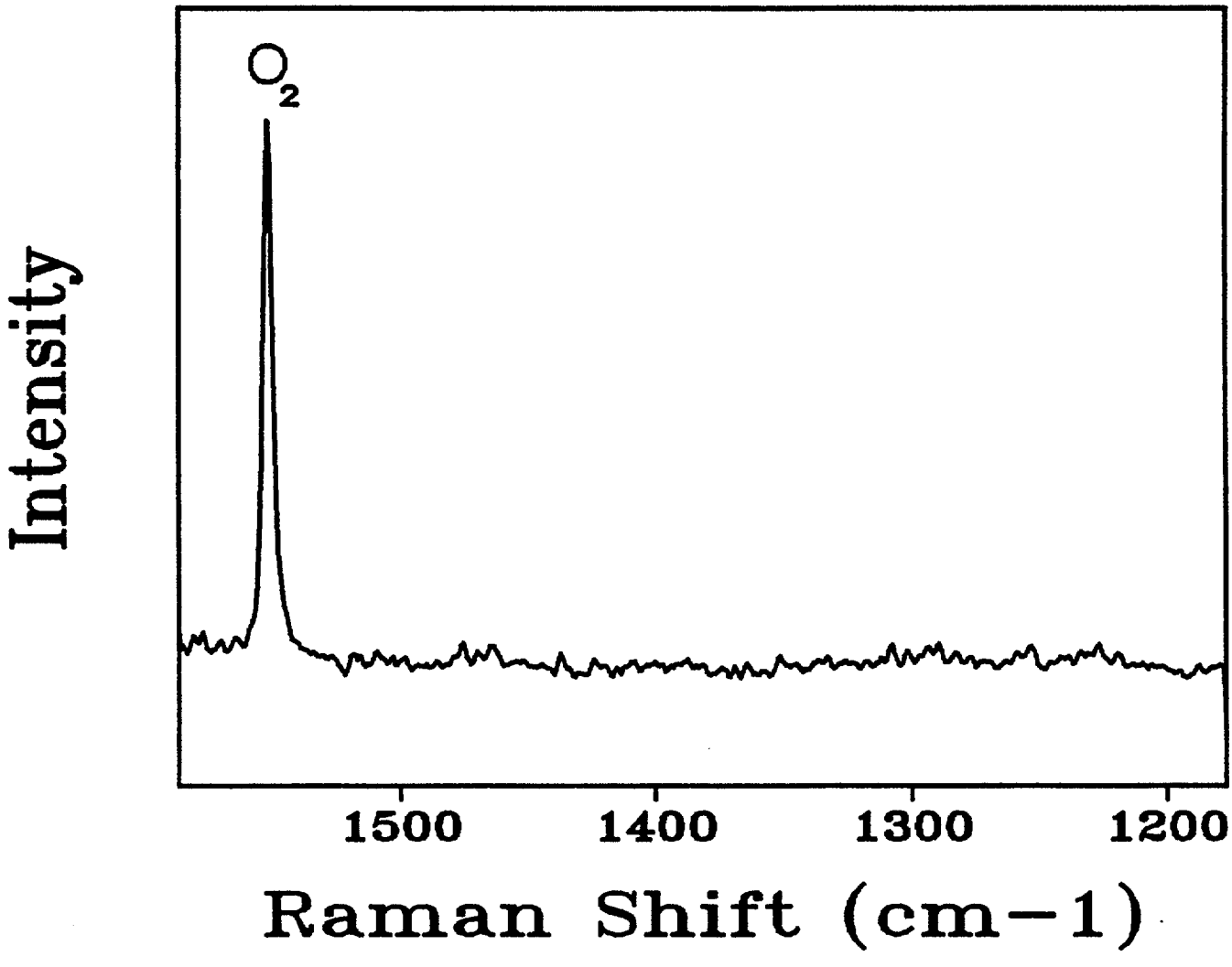

Figure 6. The Raman spectrum recorded from the vapour phase of an aqueous fluid inclusion close to pitchblende ore. It shows an oxygen band at 1552 cm^{-1} and the complete lack of CO_2 at 1388 and 1285 cm^{-1}.

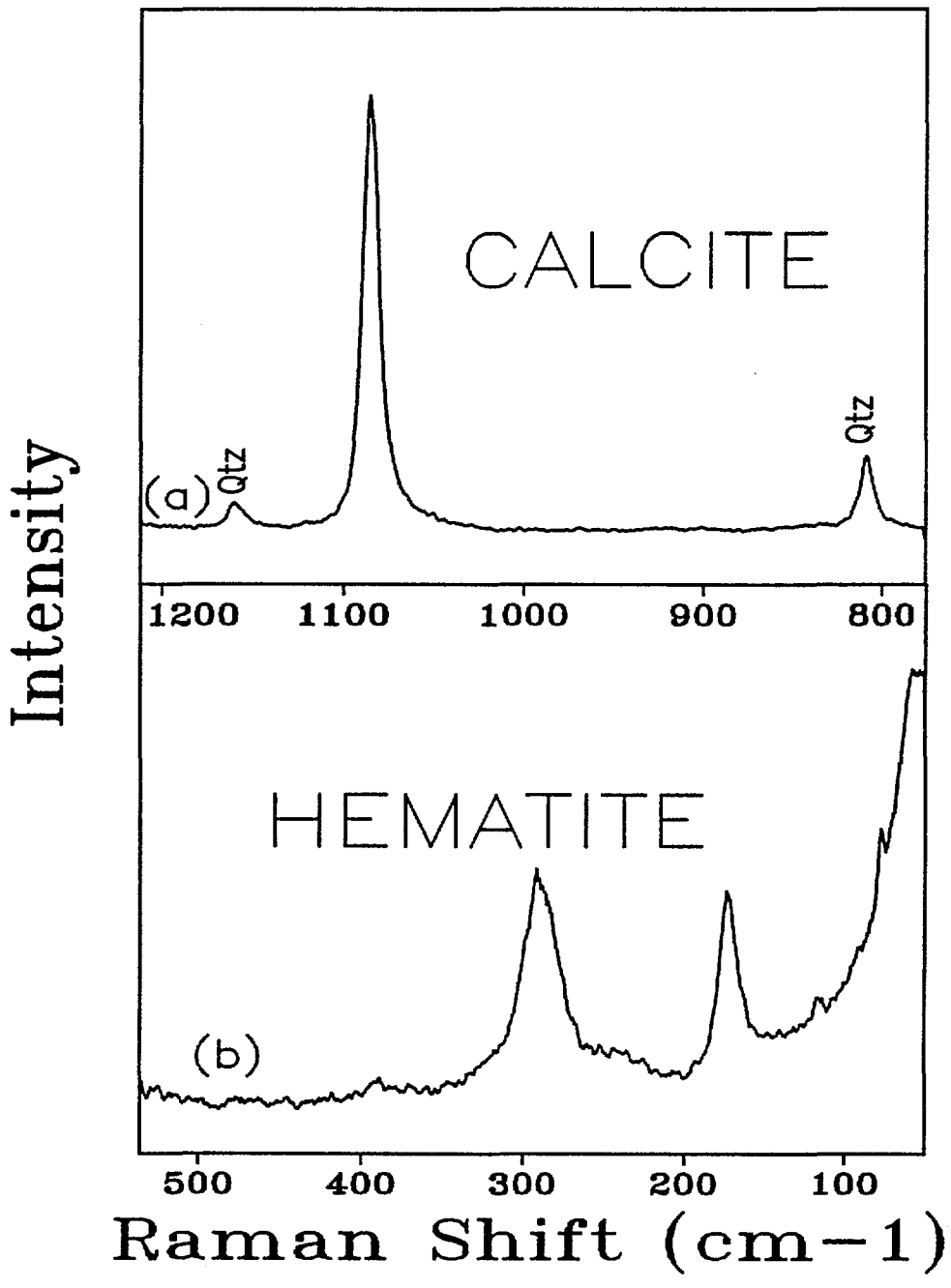

Figure 7. Raman microprobe spectra of some solids in secondary fluid inclusions from mineralised quartz veins: (a)calcite, and (b) hematite. Qtz denotes Raman bands from the host quartz.

water. Several non-ionic solids in Type C inclusions were also identified during room-temperature Raman studies (see Figure 7). The most common daughter mineral was calcite and fine bright orange crystals, confirmed to be hematite. A small zone of minor copper mineralisation also exists at Coronation Hill, and inclusions from this region had either one to three daughter minerals or a mass of clear crystals, some of which were identified by Raman spectroscopy as white mica, most probably sericite (Figure 8). The Raman microprobe also detected graphite in some of the fluid inclusions in the deeper carbonate veins, thus indicating a reduced fluid at depth.

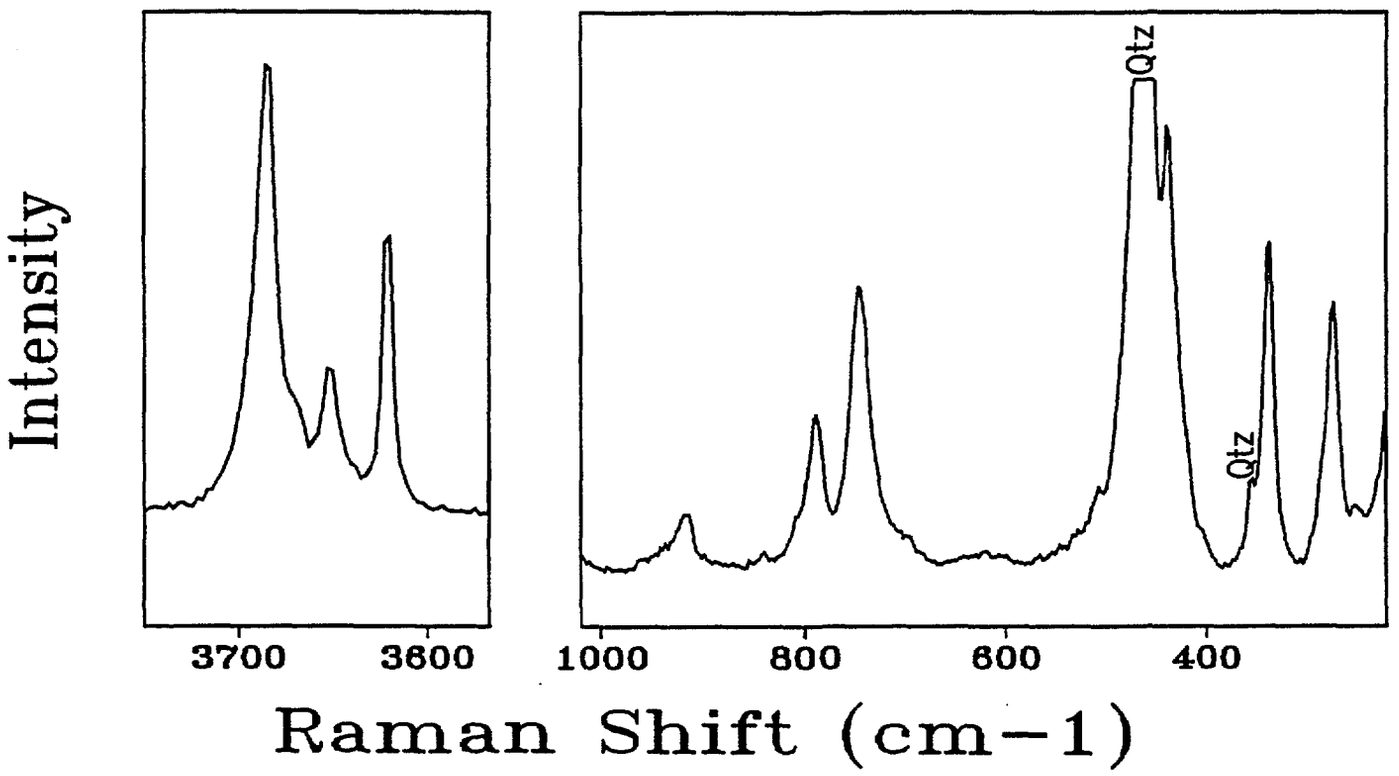

Figure 8. The Raman spectrum of white mica found in some secondary fluid inclusions near zones of copper mineralisation. Qtz denotes Raman bands from the host quartz.

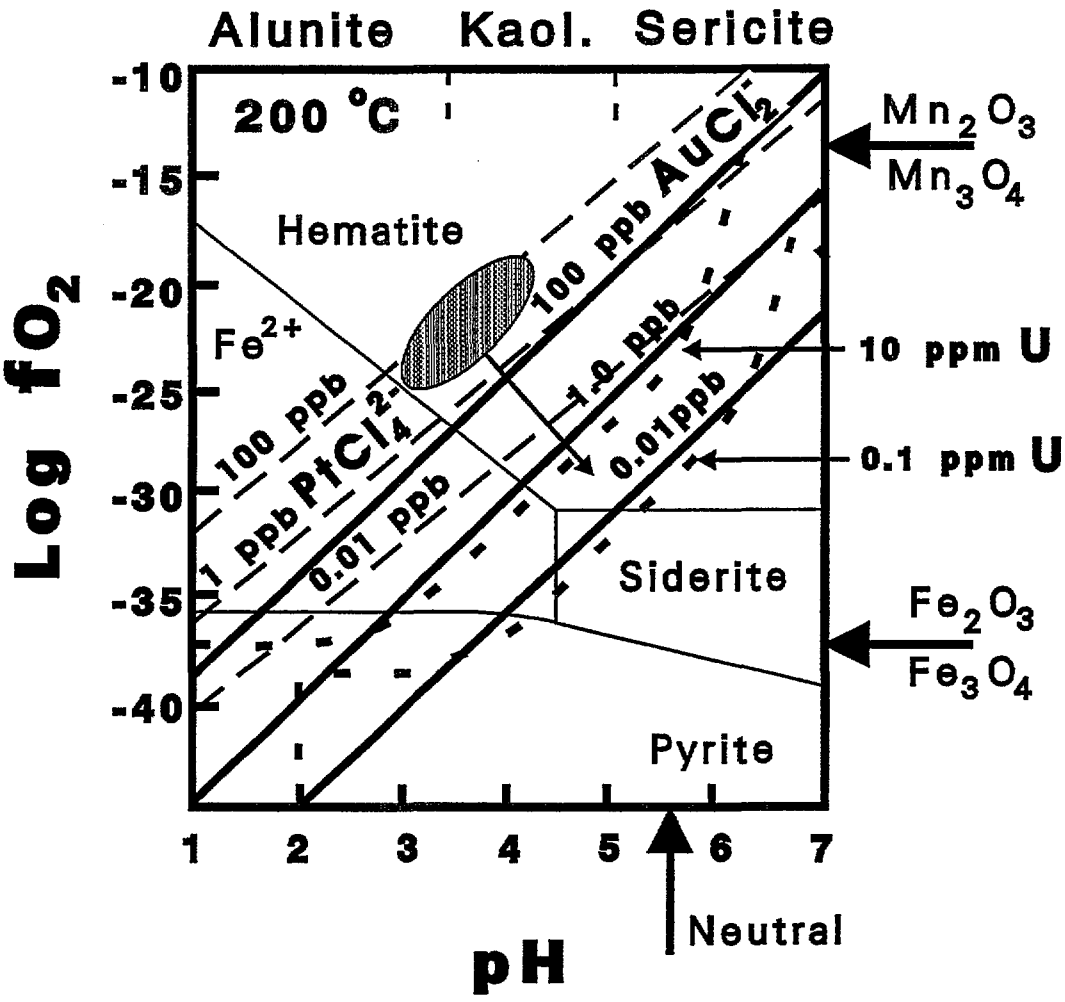

Figure 9. Log fO_2 – pH diagram showing the distribution of iron phases, and the solubility of uranium oxides, $AuCl_2^-$ and $PtCl_4^{2-}$ in solution at 200° C. Heavy arrows on the right ordinate marks the position of the hematite + magnetite, and Mn_3O_4 + Mn_2O_3, redox buffer assemblages. The hatched region indicates the possible pH and oxidation state of the original ore fluid and the light arrow shows a possible reaction path.

OXYGEN ISOTOPES

Oxygen isotope data from the quartz and carbonate veins at Coronation Hill have an average of 13.3 $^0/_{00}$, varying by 5 $^0/_{00}$. The $\delta^{18}O$ values for the fluid calculated at the average homogenisation temperature of each sample range from -1.7 to -6.6 $^0/_{00}$, with an average of -3.6 $^0/_{00}$. The negative $\delta^{18}O$ values of the fluids are incompatible with a magmatic or metamorphic origin, quite conclusively indicating that meteoric water is the main component of the mineralising fluid.

MINERALISATION MECHANISMS

The fluid inclusion and isotope data place important constraints on ore deposit models for Coronation Hill. The fluid inclusions demonstrate that the ore fluid was very saline with an unusually high $CaCl_2$ content and that mineralisation probably occurred from a boiling fluid at around 140°C. Furthermore, the fluids were highly oxidised and the replacement of earlier chlorite by hematite is commonly observed throughout the deposit. These characteristics and the isotope data show that Coronation Hill is unlike the typical epithermal precious and base-metal deposits, with a completely different element and mineral association, and are usually formed at higher temperatures from very low salinity fluids.

Thermodynamic calculations indicate that, under the conditions described above, Au and PGE transport would have been dominantly as chloride complexes (see Figure 9). The solubility of $AuCl_2^-$ at 200°C has been calculated by Jaireth (1988) from the data of Helgeson (1969). The solubility of $PtCl_4^{2-}$ has been calculated by thermodynamic interpolation between the low temperature data of Barner & Scheuerman (1978) and the empirical geothermal data of McKibben & others (1990). This data has been superimposed on the log fO_2 vs pH diagram for uranium, modified from Romberger (1984) in order to allow a simultaneous comparison of these three chemical systems.

The acidic, highly oxidised mineralising fluids originated at conditions (depicted by the hatched field in Figure 9) and descended into the faulted Early Proterozoic sequence of igneous intrusives and volcaniclastics, and carbonaceous units of the Koolpin Formation. Fluid interaction with the feldspathic rocks and periodic boiling initially caused an increase in pH to buffered values around pH 5 and a moderate decrease in log fO_2. The above process, shown by the small arrow in Figure 9, could have resulted in the deposition of significant quantities of Au and PGEs, but would have kept most of the uranium in solution. This mechanism is thought to have been responsible for the Au-PGE mineralisation with little or no uranium. The U-Au-PGE mineralisation occurs near the unconformity between the Lower Proterozoic sequence and the overlying Coronation sandstone. The fluid inclusion data indicate that this type of mineralisation resulted form a more efficient reduction of the oxidised brine, probably by mixing with reduced fluids originating from the carbonaceous units below the unconformity.

ACKNOWLEDGEMENTS

The authors acknowledge the partners in the Coronation Hill Joint Venture for their permission to publish this data. We would also like to thank Lesley Wyborn for initiating the fluid inclusion study and for supplying data and other advice during the course of this work. Similarly, D.J. Gilbert (BHP-Minerals Exploration), R.K. Valenta (Monash University), C.A. Heinrich (BMR), S-S. Sun (BMR) and M. Solomon (BMR) are thanked for helpful discussions and comments. The oxygen isotope analyses were carried out by Anita Andrew from CSIRO Division of Exploration Geoscience.

REFERENCES

Ballhaus, C.G., and Stumpfl, E.F., 1986, Sulfide and platinum mineralization in the Merensky reef: Evidence from hydrous silicates and fluid inclusions: Cont. Mineral. Petrol, v. 94, p. 193-204.

Barner, H.E., and Scheuerman, R.V., 1978, Handbook of thermochemical data for compounds and aqueous species: New York, John Wiley, 156p.

Bodnar, R.J., Reynolds, T.J., and Kuehn, C.A., 1985, Fluid-inclusion systematics in epithermal systems, *in* Berger, B.R., and Bethke, P.M., eds.: Rev. Econ. Geol., v. 2, p. 73-97.

Carville, D.P., Leckie, J.F., Moorhead, C.F., Rayner, J.G., and Durbin, A.A., 1990, Coronation Hill gold-platinum-palladium deposit, *in* Hughes, F.E., ed., Geology of the Mineral Deposits of Australia and Papua New Guinea: Australasian Institute of Mining and Metallurgy Monograph 14, p. 759-762.

Carville, D.P., Leckie, J.F., Moorhead, C.F. and Rayner, J.G., 1991, Coronation Hill unconformity related gold platinum palladium prospect, Northern Territory, *in* World Gold '91, Cairns, April 21-25, p. 287-293.

Dillon-Leitch, H.C., Watkinson, D.H., and Coats, C.J.A., 1986, Distribution of platinum- group elements in the Donaldson West deposit, Cape Smith belt, Quebec: Econ. Geol., v. 81, p. 1147-1158.

Fisher, W.J., 1969, Mining practice in the South Alligator Valley: Atomic Energy in Australia, v. 12, p.25-40.

Foy. M., 1975, South Alligator River uranium deposits: Australasian Inst. Mining Metallurgy Mon. 5, p. 304-310.

Fuchs, A.W., and Rose, A.W., 1974, The geochemical behaviour of platinum and palladium in the weathering cycle in the Stillwater Complex, Montana: Econ. Geol., v. 69, p. 332-346.

Gilbert, D.J., 1987, Mineralogical occurrence and texture of gold, platinum group minerals and other phases in heavy liquid fractions and diamond drill core samples, from Coronation Hill, Northern Territory: Petrology Section report No. MRL204, BHP Melbourne Research Laboratories, v.1, 64p.

Greenhalgh, D., and Jeffery, P.M., 1959, A contribution to the pre-Cambrian chronology of Australia: Geochim. Cosmochim. Acta, v. 16, p. 39-57.

Gustafson, L.B., and Curtis, L.W., 1983, Post-Kombolgie metasomatism at Jabiluka, Northern Territory, Australia, and its significance in the formation of high-grade uranium mineralization in lower Proterozoic host rocks: Econ. Geol., v. 78, p. 26- 56.

Helgeson, H.C., 1969, Thermodynamics of hydrothermal systems at elevated temperatures and pressures: Amer. J. Sci., v. 267, p. 729-804.

Hewett, D.F., 1956, Geology and mineral resources of the Ivanpah quadrangle, California and Nevada: U.S. Geol. Survey Prof. paper 275, 172p.

Jaireth, S., 1988, Hydrothermal transport of platinum and gold in unconformity-related uranium deposits - a preliminary thermodynamic investigation: Bureau of Mineral Resources, Geology and Geophysics, Australia, Rec. 1988/9, 55p.

Kucha, H., 1982, platinum-group metals in the Zechstein copper deposits, Poland: Econ. Geol., v. 77, p. 1587-1591.

Mathez, E.A., 1989, Interactions involving fluids in the Stillwater and Bushveld complex: observations from the rocks. *in* Whitney, J.A., and Naldrett, A.J., eds., Ore Deposits Associated with Magmas. Rev. Econ. Geol., v. 4, p. 167-179.

McKibben, M.A., Williams, A.E., and Hall, G.E.M., 1990, Solubility and transport of platinum-group elements and Au in saline hydrothermal fluids: Constraints from geothermal brine data: Econ. Geol., v. 85, p. 1926-1934.

Mihalik, P., Jacobson, J.B.E., and Hiemstra, S.A., 1974, Platinum-group minerals from a hydrothermal environment: Econ. Geol., v. 69, p. 167-179.

Needham, R.S., 1987, Review of mineralisation of the South Alligator Valley: Bureau of Mineral Resources, Geology and Geophysics, Australia, Rec. 1987/52, 68p.

Needham, R.S., and Stuart-Smith, P.G., 1987, Coronation Hill U-Au mine, South Alligator Valley, Northern Territory: an epigenetic sandstone-type deposit hosted by debris- flow conglomerate: BMR Journal of Australian Geology & Geophysics, v. 10, p. 121- 132.

Needham, R.S., Crick, I.H., and Stuart-Smith, P.G., 1980, Regional geology of the Pine Creek geosyncline, *in* Ferguson, J., and Golbey, A., eds., Uranium in the Pine Creek geosyncline: Vienna, Internat. Atomic Energy Agency, p. 1-22.

Needham, R.S., Stuart-Smith, P.G., and Page, R.W., 1988, Tectonic evolution of the Pine Creek Inlier, Northern Territory: Precambrian Research, v. 40/41, p. 543-564.

Nyman, M.W., Sheets, R.W., and Bodnar, R.J., 1990. Fluid inclusion evidence for the physical and chemical conditions associated with intermediate temperature PGE mineralization at the New Rambler deposit, southeastern Wyoming: Canadian Mineralogist, v. 28, p. 629-638.

Ottemann, J. and Augustithis, S.S., 1967, Geochemistry and origin of "platinum-nuggets" in lateritic covers from ultrabasic rocks and birbirites of W. Ethiopia: Mineral. Deposita, v. 1, p. 269-277.

Plimer, I.R., and Williams, P.A., 1988, new mechanisms for the mobilization of the platinum-group elements in the supergene zone, *in* Pritchard, H.M., Potts, P.J., Bowles, J.F.W., and Cribb, S.J., eds., Geo-Platinum 87, Elsevier, London, p.83-92.

Romberger, S.B., 1984, Transport and deposition of uranium in hydrothermal systems at temperatures up to 300°C; geological implications, *in* de Vivo, B., *et al.,* eds., Uranium geochemistry, mineralogy, geology, exploration and resources: London, Inst. Min. and Metall., p. 12-17.

Stumpfl, E.F., 1974, The genesis of platinum deposits: Further thoughts: Minerals Sci. Eng., v. 6, p. 120-141.

Volborth, A., and Housley, R.M., 1984, A preliminary description of complex graphite, sulfide, arsenide, and platinum-group element mineralization in a pegmatoid pyroxenite of the Stillwater Complex, Montana, U.S.A.: Tschermaks Mineralog. Petrog. Mitt., v. 33, p. 213-130.

Warren, R.G., and Kamprad, J.L., 1990, Mineralogical, petrographic and geochemical studies in the South Alligator Region. Pine Creek Inlier, N.T.: Bureau of Mineral Resources, Geology and Geophysics, Australia, Rec., 1990/54, 113p.

Watkinson, D.H. and Melling, D.R., 1992, Hydrothermal origin of platinum-group mineralization in low-temperature copper sulfide-rich assemblages, Salt Chuck intrusion, Alaska: Econ. Geol., v. 87, p. 175-184.

Wilde, A.R., and Wall, V.J., 1987, Geology of the Narbarlek uranium deposit, Northern Territory, Australia: Econ. Geol., v. 82, p. 1152-1168.

Wilde, A.R., Bloom, M.S., and Wall, V.J., 1989a, Transport and deposition of gold, uranium, and platinum-group elements in unconformity-related uranium deposits: Econ. Geol. MON. 6, p. 637-650.

Wilde, A.R., Mernagh, T.P., Bloom, M.S., and Hoffmann, C.F., 1989b, Fluid inclusion evidence on the origin of some Australian unconformity-related uranium deposits: Econ. Geol., v. 84, p. 1627-1642.

Wray, E.M., Ayres, D.E., and Ibrahim, H., 1985, Geology of the Mid-west uranium deposit, Northern Saskatshewan: Canadian I.M.M., v. 32, p. 54-66.

Wyborn, L.A.I., Valenta, R.K., Jagodzinski, E.A., Whitaker, A., Morse, M.P. and Needham, R.S., 1991, A review of the geological, geophysical and geochemical data of the Kakadu Conservation Zone as a basis for estimating resource potential: Bureau of Mineral Resources Geology and Geophysics, Australia, Report to Resource Assessment Commission, 290p.

Ypma, P.J.M., and Fuzikawa, K., 1980, fluid inclusion and oxygen isotope studies of the Narbarlek and Jabiluka uranium deposits, Northern Territory, Australia, *in* Ferguson, J. and Golbey, A., eds., Uranium in the Pine Creek geosyncline: Vienna, Internat. Atomic Energy Agency, p. 375-395.

TABLE 1 SAMPLES FOR FLUID INCLUSION STUDIES

Type A = Vapour rich (>25 vol. % vap.) inclusions
Type B = Undersaturated aqueous inclusions
Type C = Saturated (i.e. 3 phase) inclusions
Type D = Liquid only aqueous inclusions
Type E = CO2 rich inclusions

SECTION A MINERALISED SAMPLES

90127004 Quartz/chlorite microveins (1-3 mm) in quartz feldspar porphyry
No usable fluid inclusions in quartz microveins
Many fluid inclusions observed in quartz phenocrysts in the porphyry
1-30 micron inclusions, irregular-rounded-negative crystal shapes
Mostly secondary in healed micro-fractures, evidence of necking
Consistent L/V ratios in some micro-fractures for Types II and IV
Types A, B and C observed in quartz phenocrysts

Sample Number	Incl Type	Size microns	Vol % CO2 (L+V)	Vol % H2O vap.	Vol % solids	Tn ice	Te ice	Tm ice	Salinity Wt%CaCl2	Tm CaCl2	Th	Td	Comments
901270004	B	10		5				-47.8	30		116		Th(L)
DDH31/47.80	C	15		5	1						118.5	326.2	in porph
	B	5		5				-47.3	30.2		115.6		S in qtz phenocryst in porphyry Th(L)
	C	10		5	2	-54	-87.6	-35.1	32		136.5	118.3	S in qtz phenocryst in porphyry Th(L)
	C	20		5	2			-35.5	32.3		141.3	307.8	S in qtz phenocryst in porphyry Th(L)
	B	10		5			-84.3	-52.2	30		39.8		S in qtz phenocryst in porphyry Th(L)
	C	15		5	2			-52.8	30		141.1		S in qtz phenocryst in porphyry Th(L)
	B	15		5				-52.2	30		105.6		S in qtz phenocryst in porphyry Th(L)
	C	10		5	10		-84.3	-51.9	30		115.7		S in qtz phenocryst in porphyry Th(L)
	C	10		5	2			-52.3	30		116.7		S in qtz phenocryst in porphyry Th(L)
	B	10		5			-85.2	-28.5	33.1		116.2		S in qtz phenocryst in porphyry Th(L)

901270005a Quartz vein in quartz feldspar porphyry containing visible gold.
Abundant inclusions (1-15 microns) in clear euhedral quartz in large (<20 mm) and small (<3 mm) veins.
The inclusions are irregular to rounded. Primary inclusions occur in growth zones in euhedral quartz. Irregular inclusions may be secondary.
Types A, B and D observed. Mostly Type B with consistend L/V ratios.

Sample Number	Incl Type	Size microns	Vol % CO2 (L+V)	Vol % H2O vap.	Vol % solids	Tn ice	Te ice	Tm ice	Salinity Wt%CaCl2	Tm CaCl2	Th	Td	Comments
901270005a	B	5		10		-71		-55.5	30				P in growth zone Th(L)
DDH31/123.40	B	6		10				-36.1	31.4		139.7		P in growth zone Th(L)
	B	5		10		-115	-71	-37.5	31.3				P in growth zone Th(L)
	B	4		10				-48.3	30.2		140.2		P in growth zone Th(L)
	B	3		10				-57.2	30		139.7		P in growth zone Th(L)
	B	5		10				-45	30.5		141.9		P in growth zone Th(L)
	A	8		50		-120		-8.4	11				Secondary
	A	2		35			-65	-7	10.5		188.3		Secondary Th(L)
	A	3		40		-80		-66.2	30				Secondary
	B	4		10		-67		-20.7	34.2		83.9		Secondary Th(L)
	B	6		10				-27	33.5		86.8		P in growth zone Th(L)
	B	4		15				-21.1	34		84.8		P in growth zone Th(L)
	B	10		10							86.8		P in growth zone Th(L)
	B	8		10							85.5		P in growth zone Th(L)

Sample Number	Incl Type	Size microns	Vol % CO2 (L+V)	Vol % H2O vap.	Vol % solids	Tn ice	Te ice	Tm ice	Salinity Wt%CaCl2	Tm CaCl2	Th	Td	Comments
	B	20		10		-100	-64.8	-23.9	33.5				P in growth zone Th(L)
	B	2		10							146.8		P in growth zone Th(L)
	C	5		10	2		-60.1	-16.1	34.5				P in growth zone Th(L)
	B	5		15			-44.5	-14.6	17.5		131.9		P in growth zone Th(L)
	B	5		15				-11.5	15.2		165.8		P in growth zone Th(L)
	A	3		50				-4.3	10.2				In qtz phenocrysts Th(L)
	A	4		75				-3.7	8				In qtz phenocrysts Th(L)
	B	3		10		-85		-3.8	8.2		245.6		In qtz phenocrysts Th(L)
	B	4		10				-3.6	7.8		245.6		In qtz phenocrysts Th(L)
	B	15		15		-61	-56.3	-2.5	6.1				In qtz phenocrysts Th(L)

901270006 Quartz vien in green tuffaceous siltstone.
A few small (<1-10 micron) inclusions in quartz vein.
Primary?, mostly rounded. Types A and B observed. Type B have consistent L/V ratios.

Sample Number	Incl Type	Size microns	Vol % CO2 (L+V)	Vol % H2O vap.	Vol % solids	Tn ice	Te ice	Tm ice	Salinity Wt%CaCl2	Tm CaCl2	Th	Td	Comments
901270006	A	3		60				-13.9	17.8		163		Th(L)
DDH43/7.70	B	3		5				-19.1	20.3		175.4		Th(L)
	B	2		10				-18.2	20		165.5		Th(L)
	B	3		5				-22.1	22.2		146.2		Th(L)
	A	5		40				-18	20				
	B	3		5				-19.4	20.5		118.7		Th(L)
	B	8		5			-63.2	-27.2	24		145.2		Th(L)

901270007 Carbonate vein in brecciated quartz feldspar porphyry.
Abundant irregular fluid inclusions (<1-20 microns) in carbonate vein.
Primaries observed in growth zones but most have inconsistent L/V ratios
Types A, B and D observed.

Sample Number	Incl Type	Size microns	Vol % CO2 (L+V)	Vol % H2O vap.	Vol % solids	Tn ice	Te ice	Tm ice	Salinity Wt%CaCl2	Tm CaCl2	Th	Td	Comments
901270007	B	20		20			-83.6	-46.4	28.8				
DDH29/226.5	B	8		20				-16.3	19.3		339.8		P Th(L)
	B	8		20		-85		-12.4	16.5		342.4		P Th(L)
	A	5		90				-9.6	13				
	B	10		15			-56.1	-15.6	18.3		346		P Th(L)
	B	5		10				-15	18		252.2		P Th(L)
	A	10		85				-5.4	7.5				
	B	5		15				-16.9	19		258.1		P Th(L)
	B	5		10		-80	-67.2	-15.9	18.8				
	B	5		15				-25.7	23.2		178.5		P Th(L)
	B	3		15				-14.1	17.2		202.5		P Th(L)
	B	3		15				-11.1	14.5		240.7		P Th(L)
	B	5		10				-13.1	16.3		118.9		P Th(L)
	B	2		20							340.9		P Th(L)
	A	8		60							414.4		P Th(L)
	B	6		10				-8.5	12		150.8		P Th(L)
	B	4		15							208.1		P Th(L)

901270008 Quartz vein containing visible gold (+pitchblende) on outer walls of the vein in brecciated quartz feldspar porphyry
Abundant, mostly rounded, fluid inclusions (<1-10 microns) in large vein (<15mm).
Mostly secondary with small (primary?) inclusions in growth zone.
Types A, B, C and D observed but most have inconsistent L/V ratios.

Sample Number	Incl Type	Size microns	Vol % CO2 (L+V)	Vol % H2O vap.	Vol % solids	Tn ice	Te ice	Tm ice	Salinity Wt%CaCl2	Tm CaCl2	Th	Td	Comments
901270008	A	6		50				-4.9	7.1		177.5		Th(V)
DDH49/294.10	B	8		10				-11.8	15.8		263.3		Th(L)
	A	10		80				-12.9	15.7		377.1		Th(L)
	B	5		20				-1.5	2.1		260.5		Th(L)
	B	10		25				-1.7	2.3				
	B	10		10				-1.1	1.9				
	B	20		20				-0.8	1.2				
	B	4		10		-47	-16.6	-1	1.3				
	B	8		10		-36		0	0		98.9		Th(L)
	B	5		10				0	0		153.5		Th(L)
	B	10		10		-46		-2.6	4		155.3		Th(L)
	B	10		15				-1.7	2.3		120.9		Th(L)
	B	6		10				-6.2	8.5		191.7		Th(L)
	A	5		35				-6.3	8.5		179.8		Th(L)
	A	5		35				-5.7	7		331.3		Th(L)
	A	10		60				-5.8	7.1		334.3		Th(L)
	A	5		75				-3.5	4.8		336.7		Th(L)
	B	5		10				-3.2	4.8		390.2		Th(L)
	C	5		15	5			-3.6	4.9				
	B	5		15				-5.3	6.9				
	A	5		40				-4.4	5.8		333.3		Th(L)
	A	10		60		-47		-4.3	5.8		358.4		Th(L)
	B	15		10							414.4		Th(L)
	A	10		40							193.8		Th(L)
	A	15		35							368.4		Th(L)
	B	20		10				-15	18.1				
	B	20		20		-85	-51.6	-15.5	18.5			290.4	P Th(V)
	B	5		10		-75		-14.7	18			312.7	P Th(V) Salt cystals form on freezing
	C	4		10	5	-75		-13.3	16.9				
	B	4		10				-15	18.1				
	B	4		10				-10.8	14.8			288	P Th(V)
	B	8		10		-80		-14.8	18			289.6	P Th(V)
	A	3		60			-47.8	-1.8	3				
	A	2		40				-2.6	3.5		343.7		Th(L)
	C	2		25	5			-2	3		252.3		Th(L)
	B	3		5				4.9	0		297.8		Th(L)
	A	4		40		-75		0.6	0		330.8		Th(L)
	A	3		50				0.4	0		430.2		Th(V)
	A	10		40				-0.1	0		430.2		Th(V)
	B	5		15				-3.2	3.8		376.8		Th(L)
	B	8		10				-2.8	3.5		298.6	381.8	Th(L)

901270012a Quartz/chlorite veins in quartz feldspar porphyry.
Many inclusions (<1-20 microns) with a wispy texture observed in the quartz veins.
Secondary, irregular to rounded inclusions showing evidence of necking.
Types A, B and D observed. Inconsistent L/V ratios.

Sample Number	Incl Type	Size microns	Vol % CO2 (L+V)	Vol % H2O vap.	Vol % solids	Tn ice	Te ice	Tm ice	Salinity Wt%CaCl2	Tm CaCl2	Th	Td	Comments
901270012a	C	5		30	1						434.2		Th(L)
DDH33/51.80	A	10		50				-48.8	30.2				
	A	10		40				-45.3	30.6		394		Th(L)
	A	10		40				-44.9	30.8		370.2		Th(L)
	A	10		40				-47.5	30.2		445.5		Th(L)
	B	20		5				2.7	37.1		450.5		Th(L)
	A	10		40				-43.1	31.1		390.9		Th(L)
	A	10		40							392.8		Th(L)

901270013a 5mm quartz vein in quartz feldspar porphyry.
Abundant small (<1-10 micron) inclusions in quartz vein with wispy texture.
Secondary, irregular with evidence of necking and inconsistent L/V ratios.
Types A, B, D and C (rare) were observed.

Sample Number	Incl Type	Size microns	Vol % CO2 (L+V)	Vol % H2O vap.	Vol % solids	Tn ice	Te ice	Tm ice	Salinity Wt%CaCl2	Tm CaCl2	Th	Td	Comments
901270013a	B	10		5		-66	-52	1.2	0		177.5		Th(L)
DDH34/69.60	B	8		5							210.1		P Th(L)
	A	15		40				-0.5	0.8				
	B	10		20							299.5		P Th(L)
	C	20		10	2			9.2	13		255.2		Th(L)
	A	6		75				-0.2	0.3				
	B	5		10			-58.4	-22.5	22.1		156.9		Th(L)
	C	5		5	2		-56.6	-20.6	21.5		171.8		Th(L)
	B	3		5				-20.3	21.3		146.4		Th(L)
	B	8		5				-19.9	21		147.9		Th(L)
	B	8		10				-30.9	26		297.1		Th(L)

901270014b Quartz vein in quartz feldspar porphyry.
Many relatively large (<1-50 micron) inclusions with wispy texture observed in quartz vein.
Inclusions near colloidal hematite bands may be primary.
Mostly irregular inclusions but Type II have consistent L/V ratios in a single micro-fracture.
Types A and B observed.

Sample Number	Incl Type	Size microns	Vol % CO2 (L+V)	Vol % H2O vap.	Vol % solids	Tn ice	Te ice	Tm ice	Salinity Wt%CaCl2	Tm CaCl2	Th	Td	Comments
901270014b	C	20		5	2			-18.6	34.1		195.3		Th(L)
DDH34/73.50	B	15		5				-18.8	34.1		147.5		Th(L)
	B	20		5				-18.8	34.1		148.8		Th(L)
	B	25		5				-18.7	34.1		153.6		Th(L)
	B	10		5				-19	34		157.8		Th(L)
	B	8		5				-15.8	34.5		155		Th(L)
	B	8		5							158.4		Th(L)
													Different micro-fracture
	A	8		60				-0.2	0.3		347.9		Th(L)
	A	5		40				-3.3	5.4		346.1		Th(L)
	A	5		40				-2.7	4.4		360.6		Th(L)
	A	8		50				-3	5		361.3		Th(L)

Sample Number	Incl Type	Size microns	Vol % CO2 (L+V)	Vol % H2O vap.	Vol % solids	Tn ice	Te ice	Tm ice	Salinity Wt%CaCl2	Tm CaCl2	Th	Td	Comments
	A	8		90				-3.2	5.3				
	B	5		5							233.6		Th(L)
	B	5		5							291.7		Th(L)

901270016a Quartz micro-veins (<3 mm) in quartz feldspar porphyry.
Abundant inclusions (<1-30 micron) in the quartz veins.
Primaries in growth zones but most are in trails of secondaries or pseudosecondaries.
Types A, B and C observed. Irregular to rounded with evidence of necking.
L/V ratios vary but are consistent within single micro-fractures.

Sample Number	Incl Type	Size microns	Vol % CO2 (L+V)	Vol % H2O vap.	Vol % solids	Tn ice	Te ice	Tm ice	Salinity Wt%CaCl2	Tm CaCl2	Th	Td	Comments
901270016	C	5		25	2	-125	-21.8	-6.4	11				P in growth zone
DDH37/40.40	B	5		5				-5.5	9.5		239.8		P Th(L)
	B	5		20		-125		-5.6	9.5				P Th(L)
	C	5		10		-85		-5	9.3		159		P Th(L)
	B	8		10				-5.3	9.4		223.2		P Th(L)
	C	5		10	15	-125					213.4		P Th(L)
	A	5		50				-5.5	9.5				P Th(L)
	B	15		10			-61.5	-36.7	32		108.6		P Th(L)
	B	5		10				-33	32.5				P Th(L)
	B	6		15							176.1		P Th(L)
	B	10		15		-105		-33.4	32.5				P Th(L)
	B	10		5			-60.9	-39.3	31.2		66.1		P Th(L)
	A	30		50			-78.1	-25.6	33.5				P Th(L)
	B	8		15				-23.9	33.8		142.1		P Th(L)
	C	5		10				-40.3	30.5		261.9		P Th(L)
	B	5		5				-42.2	30.2		115		P Th(L)
	A	15		50				-31	32				P Th(L)
	A	10		50				-31.7	31.8				P Th(L)
	B	5		5							201.6		P Th(L)
	B	5		5							135.3		P Th(L)
	B	5		5							66.2		P Th(L)
	B	5		5							110.8		P Th(L)
	B	10		10							262.2		P Th(L)
	B	6		5							133.9		P Th(L)
	B	20		5							118		Secondary
	B	10		10							180.4		P Th(L)
	A	10		50							383.5		Th(V)
	A	6		90							326.8		Th(V)
	A	10		50							497.3		Th(V)
	A	10		50									
	A	10		50							508.5		Critical behaviour
	B	3		5							286.3		Th(L)
	A	15		80							417.5		Th(V)

901270019 Carbonate vein (20 mm) and microveining in quartz diorite.
Few small (<1-5 micron) inclusions in veins.
Secondary, irregular, mostly decrepitated.
Type A and B (rare) observed.

Sample Number	Incl Type	Size microns	Vol % CO2 (L+V)	Vol % H2O vap.	Vol % solids	Tn ice	Te ice	Tm ice	Salinity Wt%CaCl2	Tm CaCl2	Th	Td	Comments
901270019	B	20											
DDH45/141	A	80									84		Th(V)
	A	60									430.2		Th(V)
	B	15									162.3		Th(L)
	B	25									181		Th(L)
	B	25									314.5		Th(L)
	B	25									267		Th(L)
	B	25									287.7		Th(L)
	B	25									289.8		Th(L)
	B	15						1.8	36.5		330		Th(L)

901270020 Quartz microveins (<3 mm) with visible gold in quartz diorite.
Very small (<1-5 micron) inclusions with wispy texture in quartz veins.
Secondary, mostly rounded, vapour rich Type A.

Sample Number	Incl Type	Size microns	Vol % CO2 (L+V)	Vol % H2O vap.	Vol % solids	Tn ice	Te ice	Tm ice	Salinity Wt%CaCl2	Tm CaCl2	Th	Td	Comments
901270020	D	4					-68.1	-19.5	20.6		74.5		In large qtz veins, Th(L), Nucleated bubbl
DDH94/189.35	D	4						-19.4	20.6		106.2		In large qtz veins, Th(L), Nucleated bubbl
	D	3						-18.7	20		106.1		In large qtz veins, Th(L), Nucleated bubbl
	D	3						-18.6	20		112.4		In large qtz veins, Th(L), Nucleated bubbl
	D	2				-57					120.3		In large qtz veins, Th(L), Nucleated bubbl
	D	5					-52.7				105		In large qtz veins, Th(L), Nucleated bubbl
	D	8									109.1		In large qtz veins, Th(L), Nucleated bubbl
	B	6						-19.1	20.2		101.8		In small qtz veins, Th(L)
	A	4		40							289.4		In small qtz veins, Th(V)
	B	4		25									In small qtz veins, Th(L)
	A	6		80									In small qtz veins, Th(L)
	B	8									126		In small qtz veins, Th(L)

901270021a Carbonate veinlets in brecciated green tuffaceous siltstone.
A few, small (<1-10 micron) inclusions in micro-fractures in the veinlets.
Pseudosecondary to secondary irregular to rounded inclusions, some showing evidence of necking.
Types A and B observed with Type B having consistent L/V ratios.

Sample Number	Incl Type	Size microns	Vol % CO2 (L+V)	Vol % H2O vap.	Vol % solids	Tn ice	Te ice	Tm ice	Salinity Wt%CaCl2	Tm CaCl2	Th	Td	Comments
901270021a	B	4		5		-50					136.4		Th(L)
DDH98/285.45	B	5		5							141.3		Th(L)
	B	2		5							121.2		Th(L)
	B	3		5							139.6		Th(L)

901270025a Quartz veinlets in quartz feldspar porphyry.
Abundant primary inclusions (<1-20 micron) present mostly in growth zones or cores of quartz crystals.
Most are irregular to rounded and show evidence of necking and only a few micro-fractures have consistent L/V ratios.
Types A, B and D are observed.

Sample Number	Incl Type	Size microns	Vol % CO2 (L+V)	Vol % H2O vap.	Vol % solids	Tn ice	Te ice	Tm ice	Salinity Wt%CaCl2	Tm CaCl2	Th	Td	Comments
901270025a	B	10		5		-90	-55.4	-16.1	19.1		107.4		P in Qtz core Th(L)
DDH82/91.30	B	10		5		-90	-18.5	20.2	102.5				P in Qtz core Th(L)
	B	5		10			-17.6		19.8		105.9		P in Qtz core Th(L)
	B	8		5			-49.8	-18.5	20		53.6		P in Qtz core Th(L)
	B	15		5							121.4		P in Qtz core Th(L)
	B	3		5				-9.9	14.1		136.5		P in Qtz core Th(L)
	B	4		5				-14.2	17.5		100.9		P in Qtz core Th(L)
	B	20		5			-61	-8.7	12.4		84.9		P Nucleated bubble on freezing
	B	10		5			-69	-51.9	30		67.7		P Nucleated bubble on freezing
	B	8		10			-50	-22.3	22.5		156.3		P in Qtz core Th(L)
	A	5		50				-16.7	19.3		142.4		P in Qtz core Th(L)
	B	6		5			-80	-21.3	21.7		143.5		P in Qtz core Th(L)
	B	5		5			-100	-21.3	21.7		174.6		P in Qtz core Th(L)
	B	6		5				-21.4	21.7		144.9		P in Qtz core Th(L)
	B	3		5				-21.3	21.7				
	C	4		5	2			-18.6	20.1				
	B	10		10		-70	-67.4	-17	19.2				
	B	5		10				-19.1	20.9		166.2		
	B	3		10				-1.6	2.7		265		Qtz phenocryst in porphyry
	B	2		10				-0.6	1		199.7		Qtz phenocryst in porphyry
	B	10		10				-1.7	2.9		175.8		Qtz phenocryst in porphyry
	B	5		10				-0.5	0.8		276.5		Qtz phenocryst in porphyry
	A	6		60				-3.5	5.7		340.7		Qtz phenocryst in porphyry
	B	4		10				-1.2	2.1		198.9		Qtz phenocryst in porphyry
	B	2		10				-1.1	2		265.9		Qtz phenocryst in porphyry
	A	10		35				-3.3	5.4		352.4		Qtz phenocryst in porphyry
	A	10		35				-3.4	5.6		255.8		Qtz phenocryst in porphyry
	C	10		5				-0.8	1.3		189.6		Qtz phenocryst in porphyry

901270026a Carbonate veinlets in diorite.
Mostly small inclusions (<1-30 microns) in carbonate veins.
Mostly secondary, rounded to negative crystal shped with consistent L/V ratios in only a few micro-fractures.
Types A and B most common. Two rare Type E inclusions were also observed.

Sample Number	Incl Type	Size microns	Vol % CO2 (L+V)	Vol % H2O vap.	Vol % solids	Tn ice	Te ice	Tm ice	Salinity Wt%CaCl2	Tm CaCl2	Th	Td	Comments
901270026	B	10		5				-27.9	33		130.6		P Th(L)
DDH82/198.70	E	8	90					-45.6	30.5				P Th(L)
	B	20		5				-22.3	34		131.5		P Th(L)
	B	6		5				-10.8	35.5		131.6		P Th(L)
	B	10		10				-9.4	36		125.5		P Th(L)
	A	15		50				-23.2	33.8				
	B	10		10				-44	30.3		131.2		P Th(L)
	B	20		5				-23.6	33.7		121.7		P Th(L)
	B	20		5				-22.9	33.8		133.1		P Th(L)
	B	5		5				-22.6	33.9		137.2		P Th(L)
	B	10		5				-42.6	30.5		186.8		P Th(L)
	B	15		5				-41.9	30.6		157.7		P Th(L)
	B	10		5				-42.7	30.8		157.3		P Th(L)

Sample Number	Incl Type	Size microns	Vol % CO2 (L+V)	Vol % H2O vap.	Vol % solids	Tn ice	Te ice	Tm ice	Salinity Wt%CaCl2	Tm CaCl2	Th	Td	Comments
	B	6		5				-50	30		128.3		P Th(L)
	C	5		5				-38	31.2		141.2		P Th(L)
	A	10		75				-50.8	30				
	B	5		5				-44.2	30.3		155.6		P Th(L)
	B	30		5				-23.4	33.5		190.6		P Th(L)

901270028 Brecciated zone in quartz with anastamosing quartz veins.
Only a few small (<1-10 micron) inclusions in quartz veins.
Mostly irregular, secondary inclusions and only a few had consistent L/V ratios in individual micro-fractures.
Only Type B observed.

Sample Number	Incl Type	Size microns	Vol % CO2 (L+V)	Vol % H2O vap.	Vol % solids	Tn ice	Te ice	Tm ice	Salinity Wt%CaCl2	Tm CaCl2	Th	Td	Comments
901270028	B	2		5				-33.5	26.8		164.6		Th(L)
DDH89/206.95	B	4		5			-55.5	-34.9	27		138.6		Th(L)
	B	4		5				-34.7	27		192		Th(L)
	B	2		5							182.2		Th(L)
	B	2		5		-85		-19.6	20.9		238.1		Th(L)
	B	5		10				-12.2	16.2		294.5		Th(L)
	B	5		5				-12.7	16.5		193.4		Th(L)
	B	3		10				-12.4	16.3		289.4		Th(L)

901270030 Brecciated quartz veinlet (10 mm) in intensely brecciated green tuffaceous siltstone. Hematite outlining quartz veinlets.
Mostly very small inclusions (<1-20 micron) with the rare large inclusions occurring near the hematite.
Secondary, irregular inclusions with consistent L/V ratios.
Only Type B observed.

Sample Number	Incl Type	Size microns	Vol % CO2 (L+V)	Vol % H2O vap.	Vol % solids	Tn ice	Te ice	Tm ice	Salinity Wt%CaCl2	Tm CaCl2	Th	Td	Comments
901270030	B	20		5		-70	-62	-25.1	24.4		167.3		Th(L)
DDH18/149.50	B	5		5				-25.4	24.5		166.2		
	B	30		5			-63	-23.7	22.8		147.2		
	B	5		5		-70		-22.8	22.3		167.1		
	B	6		5			-56	-22.2	22		146.8		
	B	5		5		-71		-16.4	19.2		133.9		
	B	5		5			-54	-22.4	22.1		146.6		
	B	3		5				-11.1	15				P Growth zone in qtz crystal Th(L)
	B	8		5		-60		-11.7	15.4		206.6		P Growth zone in qtz crystal Th(L)
	B	6		5				-11.4	15.2		162.6		P Growth zone in qtz crystal Th(L)
	B	8		5		-60		-10.8	14.9		155.1		P Growth zone in qtz crystal Th(L)
	B	7		5							143.2		P Growth zone in qtz crystal Th(L)
	B	3		5							158.9		P Growth zone in qtz crystal Th(L)
	B	2		5							132.8		P Growth zone in qtz crystal Th(L)

901270034 Irregular quartz veinlet in green tuffaceous siltstone.
Many very small inclusions (<1-10 microns) in quartz veinlets.
Secondary, rounded to negative crystal inclusions with variable L/V ratios.
Mostly Type I with rare Type II also observed.

Sample Number	Incl Type	Size microns	Vol % CO2 (L+V)	Vol % H2O vap.	Vol % solids	Tn ice	Te ice	Tm ice	Salinity Wt%CaCl2	Tm CaCl2	Th	Td	Comments
901270034	B	5		25				-1.8	3		332.8		Th(L)
DDH23/19.90	A	3		90							382.7		Th(V)
	B	5		5		-30	-48	-24.7	23.8		119.7		Th(L)

901270036 Massive quartz veinlet in green tuffaceous siltstone with some quartz crystal lined vugs.
Abundant, small (<1-20 micron) inclusions in veinlet. Primaries occur in growth bands in vuggy quartz.
Inclusions are irregular to negative crystal in shape with variable L/V ratios.
Types A and B observed.

Sample Number	Incl Type	Size microns	Vol % CO2 (L+V)	Vol % H2O vap.	Vol % solids	Tn ice	Te ice	Tm ice	Salinity Wt%CaCl2	Tm CaCl2	Th	Td	Comments
901270036	B	8		5				-3.9	5.3		234.2		P Th(L) in growth zone on outer rim
DDH25/21.80	B	4		10				-3.8	5.3		236		P Th(L) in growth zone on outer rim
	B	5		10		-46		-3.8	5.3		254.9		P Th(L) in growth zone on outer rim
	B	3		10				-4.2	5.8		129.4		P Th(L) in growth zone
	B	2		5				-23.8	22.9		131.3		P Th(L) in growth zone
	B	3		5				-18.3	22.1		117.2		P Th(L) in growth zone
	B	4		10				-25.6	23.2		97.3		P Th(L) in growth zone
	B	10		5				-19.9	21		134.3		P Th(L) in growth zone
	B	5		5				-24.8	23.1		133.8		P Th(L) in growth zone
	B	3		5				-25.3	23.2		134		P Th(L) in growth zone
	B	2		5				-32.1	26		133.3		P Th(L) in growth zone
	B	4		5				-26.9	24.2		132.4		P Th(L) in growth zone

901270038 White quartz veinlets in intensely altered and hematised quartz feldspar porphyry,
with yellow flecks of clay. Some vugs lined with quartz.
Abundant very small, secondary inclusions (<1-20 micron) with irregular to rounded shapes.
Types A, B, C and D are observed. Type A are most abundant with consistent L/V ratios observed in Type C.

Sample Number	Incl Type	Size microns	Vol % CO2 (L+V)	Vol % H2O vap.	Vol % solids	Tn ice	Te ice	Tm ice	Salinity Wt%CaCl2	Tm CaCl2	Th	Td	Comments
901270038	C	10		5	5		-73	-46	30.2		90.4		Th(L)
DDH27/126.05	C	10		5	2	-78	-83	-48.3	30.1		113.9		Th(L)
	B	10		5			-63	-39.9	31		88.8		Th(L)
	C	5		5	2			-41.9	30.8		93		Th(L)
	C	6		5	2			-47.3	30.1		84.9		Th(L)
	C	8		5	2			-46.4	30.2		87.7		Th(L)
	A	10		40				-23.4	22.2		415.1		Th(L)
	A	5		50				-23.1	22.1		325.7		Th(L)
	A	6		50				-23.3	22.2		343.7		Th(L)
	C	5		5	2			-48.5	30.1				
	C	5		10	2			-47.6	30.1				

901270043 White brecciated quartz vein (10 mm) in brecciated and altered green tuffaceous siltstone.
Abundant inclusions (<1-20 micron) observed and dominated by Type I inclusions.
Inclusions are secondary and irregular to rounded with only Type C having consistent L/V ratios.
Types A, B, C and D are observed.

Sample Number	Incl Type	Size microns	Vol % CO2 (L+V)	Vol % H2O vap.	Vol % solids	Tn ice	Te ice	Tm ice	Salinity Wt%CaCl2	Tm CaCl2	Th	Td	Comments
901270043	B	6		5			-52	-22.4	22.1				
DDH49/290.90	B	5		10		-59	-48	-23	22.6		320		Th(L)
	A	6		80				-20.6	21.5		385.3		Th(L)
	C	4		5	1			-21.4	21.8		350		Th(L)
	B	5		5				-22	22		375		Th(L)
	B	7		10				-20.4	21.4		360		Th(L)
	A	5		90				-20.2	21.2		365.6		Th(L)

901270050 White vuggy quartz veinlet (5 mm) in altered quartz feldspar porphyry.
Abundant inclusions (<1-30 micron) in vuggy quartz.
Inclusions are secondary and irregular with evidence of necking.
Types A, B, C (with mostly hematite daughters) and D are observed.
Types B and C show consistent L/V ratios.

Sample Number	Incl Type	Size microns	Vol % CO2 (L+V)	Vol % H2O vap.	Vol % solids	Tn ice	Te ice	Tm ice	Salinity Wt%CaCl2	Tm CaCl2	Th	Td	Comments
901270050	B	5		5				-31.8	26.1		114.8		Th(L)
DDH57/109.65	A	10		45				-26.9	24.4				
	B	10		5				-30.8	25.9		68.7		Th(L)
	B	8		5		-80	-50	-31.6	26		119		Th(L)
	C	4		5	1		-48	-28.6	24.8		122.9		Th(L)
	C	3		5	2			-29.1	25		90.7		Th(L)
	B	5		5				-35	27		125.5		Th(L)
	B	5		5			-52	-35.4	27.2		125.3		Th(L)
	C	15		5	8			-29.8	25.2		122.1		Th(L)
	C	10		5	5			-29.5	25.1		90.7		Th(L)
	B	10		5		-75	-50	-28.5	24.8		121.4		Th(L)
	B	5		5		-80	-28.8	24.9	122		122		Th(L)

901270052 Vuggy, irregular quartz veinlet up tp 10 mm diameter in altered quartz feldspar porphyry (orange-red in colour).
Many inclusions (<1-20 microns) in vuggy quartz.
Secondary, irregular shaped inclusions showing evidence of necking.
Types A, B, C and D observed.

Sample Number	Incl Type	Size microns	Vol % CO2 (L+V)	Vol % H2O vap.	Vol % solids	Tn ice	Te ice	Tm ice	Salinity Wt%CaCl2	Tm CaCl2	Th	Td	Comments
901270052	B	20		5			-56	-38.2	31.6		250		Th(L) In qtz phenocryst in porphyry
DDH68/31.00	B	10		5		-46	-55	-39.3	31.4		106.8		Th(L) In qtz phenocryst in porphyry
	B	10		5			-64	-39.9	31.3		108		
	B	20		5			-65	-39.5	31.3		106.1		
	C	10		5	10			-36.9	31.3		110.4		
	C	10		5	6		-79	-43.9	30.5				Th(L) In qtz phenocryst in porphyry
	C	5		5	6		-76	-42.2	30.7				Th(L) In qtz phenocryst in porphyry
	B	10		5				-20.7	25.9		104.4		Th(L) In qtz phenocryst in porphyry

901270071 Carbonate vein (5 mm) in altered quartz diorite.
Abundant, very small (<1-5 micron) inclusions.
Mostly secondary, irregular to negative crystal shapes with consistent L/V ratios.
Types B and C observed.

Sample Number	Incl Type	Size microns	Vol % CO2 (L+V)	Vol % H2O vap.	Vol % solids	Tn ice	Te ice	Tm ice	Salinity Wt%CaCl2	Tm CaCl2	Th	Td	Comments
901270071	B	8		5							125.1		Secondary Th(L)
DDH100/299.0	B	4		5							124.6		Secondary Th(L)
	B	4		5							125.8		Secondary Th(L)
	B	4		5							125.3		Secondary Th(L)
	B	5		2							127.2		Secondary Th(L)

901270072 Carbonate vein (15 mm) in altered quartz diorite containing some sulfide minerals.
Abundant inclusions (<1-20 micron) in carbonate.
All secondary with irregular to negative crystal shapes and evidence of necking.
Types B and C observed.

Sample Number	Incl Type	Size microns	Vol % CO2 (L+V)	Vol % H2O vap.	Vol % solids	Tn ice	Te ice	Tm ice	Salinity Wt%CaCl2	Tm CaCl2	Th	Td	Comments
901270072	B	10		5			-52	-27.8	-10.2		120.1		Secondary Th(L)
DDH100/319.8	B	8		5				-10.8	14.7		302.3		Secondary Th(L)
	B	5		5				-11.3	15.1		165.4		Secondary Th(L)
	B	5		5			-53	-12.3	16.4		174.1		Secondary Th(L)
	B	5		5			-48	-12.9	16.8		96.5		Secondary Th(L)
	B	3		5				-14.8	15.8		192.1		Primary in growth zone Th(L)
	B	8		5				-10.5	14.5		150.2		Primary in growth zone Th(L)
	B	6		5				-11.9	15.9		175.6		Secondary Th(L)
	B	8		5							237.5		Secondary Th(L)
	B	6		10							305		Secondary Th(V)

901270073 Carbonate vein (10-15 mm) in altered quartz diorite.
Abundant, very small (<1-10 micron) inclusions in carbonate.
Inclusions are secondary and mostly irregular showing evidence of necking.
Types A, B and C (opaque + hematite daughters) observed. Type B have consistent L/V ratios.

Sample Number	Incl Type	Size microns	Vol % CO2 (L+V)	Vol % H2O vap.	Vol % solids	Tn ice	Te ice	Tm ice	Salinity Wt%CaCl2	Tm CaCl2	Th	Td	Comments
901270073	B	5		10			-58.1	-7.5	11.4		183.2		Secondary Th(L)
	B	3		5				-8.3	12.3				Secondary
	B	10		5				-12.1	16.1		136.6		Secondary Th(L)
	B	5		5			-45	-12.3	16.4				Secondary
	B	4		5							237		Secondary Th(L)
	B	6		5							224	237	Secondary Th(L)

BARREN SAMPLES

901270011a Carbonate veinlets in quartz diorite.
Only a few inclusions (<1-10 micron) observed.
All irregular, secondary and only Type B observed with consistent L/V ratios in individual micro-fractures.

Sample Number	Incl Type	Size microns	Vol % CO2 (L+V)	Vol % H2O vap.	Vol % solids	Tn ice	Te ice	Tm ice	Salinity Wt%CaCl2	Tm CaCl2	Th	Td	Comments
901270011a	B	5		5				-7.4	9		152		S Th(L)
DDH54/97.25	B	10		5		-66	-58.4	-7.9	9.3		153.6		S Th(L)
	B	10		5				-8.4	8.7		111		S Th(L)
	B	5		5		-57		-4	5		180.3		S Th(L)
	B	15		5				-4.3	5.1		185.5		S Th(L)
	B	20		5		-38		-3.2	4		157.8		S Th(L)
	B	5		5				-4.5	6		137.2		S Th(L)
	B	15		5				-4.7	6.2		165.2		S Th(L)

901270022b Carbonate veinlets in grey dolomite.
Abundant inclusions (<1-20 micron) in veinlets.
Primary to pseudosecondary and irregular to rounded.
Types A,B and C observed with Type B having consistent L/V ratios.

Sample Number	Incl Type	Size microns	Vol % CO2 (L+V)	Vol % H2O vap.	Vol % solids	Tn ice	Te ice	Tm ice	Salinity Wt%CaCl2	Tm CaCl2	Th	Td	Comments
901270022b	B	20		5			-60.2		42.1	20.6			
DDH100/425.60	B	15		5					40.2	16.4	187.9		P Th(L)
	B	10		5					39	11.4	133.4		P Th(L)
	B	10		5					40	15.1	200.2		P Th(L)
	C	20		5	5				40.8	15.9	227.1		P Th(L)
	B	30		10		-75	-51.1	-5.8	36				
	B	20		10				-5.5	36.1		201.8		Th(L)
	B	10		5					38	8.8	203.8		P Th(L)
	B	10		5					38.8	9.7	210.4		P Th(L)
	B	15		5		-50	-54.1		38.6	8.9			P Th(L)
	B	5		5		-50					237.5		P Th(L)
	B	30		5		-50					202.9		P Th(L)

901270023b Anastomosing carbonate veins in dolomite.
Large number of inclusions (<1-10 micron) observed in the carbonate.
Most are secondary but primaries outline growth bands. Larger inclusions in centre of late veins.
Types A, B and D observed.

Sample Number	Incl Type	Size microns	Vol % CO2 (L+V)	Vol % H2O vap.	Vol % solids	Tn ice	Te ice	Tm ice	Salinity Wt%CaCl2	Tm CaCl2	Th	Td	Comments
901270023	B	3		10			-28.4	-14.3	16.2				P in late vein Th(L)
ddh102/484.5	A	5		50				-17.4	19.2				
	A	10		50							207.7		P in late vein Th(V)
	A	3		50				-10.2	14				
	B	4		10							182.7		P in late vein Th(L)
	B	4		10				-1.4	2.5		263		P in Calcite growth zone Th(L)
	C	3		10	5			-6.1	10.5				P in Calcite growth zone Th(L)
	B	10		10				-0.7	1.5		262.3		P in Calcite growth zone Th(L)
	B	5		20				-0.9	1.8		300.8		On calcite xtal rim
	C	5		10	5			-0.9	1.8				On calcite xtal rim
	B	5		10				-1.9	4.3				On calcite xtal rim
	B	5		5				-24	22.6				

Sample Number	Incl Type	Size microns	Vol % CO2 (L+V)	Vol % H2O vap.	Vol % solids	Tn ice	Te ice	Tm ice	Salinity Wt%CaCl2	Tm CaCl2	Th	Td	Comments
	B	5		5				-21.9	22		152.4		In late vein Th(L)
	B	5		5		-47		-10.4	14.5		154.6		In late vein Th(L)
	B	5		10				-0.1	0.3		222.3		In late vein Th(L)
	A	5		60				-23.3	22.5				
	B	5		20				-15	18		219.5		In late vein Th(L)
	B	5		20							216.2		In late vein Th(L)

901270024b White quartz veinlets in quartz feldspar porphyry with visible sulfides.
Many secondary inclusions (<1-20 micron) with wispy texture plus some primaries outlining growth zones.
Inclusions were mostly rounded with coexisting Type A and B but most had inconsistent L/V ratios with evidence of necking.
Types A,B and D were observed.

Sample Number	Incl Type	Size microns	Vol % CO2 (L+V)	Vol % H2O vap.	Vol % solids	Tn ice	Te ice	Tm ice	Salinity Wt%CaCl2	Tm CaCl2	Th	Td	Comments
901270024b	A	6		75				0	0				
DDH79/23.15	A	8		75				-0.1	0.3		175.9		Th(L)
	B	5		20		-47		-0.6	1.5				
	A	10		70				-0.1	0.3				
	A	15		70				-0.7	1.7		215.4		Th(L)
	B	5		20				-0.3	0.8		231.5		Th(L)
	B	3		2				-0.2	0.5		234.9		Th(L)
	B	5		10				-0.5	1		279.5		Th(L)
	A	5		75				-0.4	0.9		316.1		Th(L)
	A	15		50				-0.5	1		347.4		Th(L)
	C	10		5	5			-0.6	1.5		310.9		Th(L)
	B	15		10				-1	4.5		236		Th(L)
	C	5		10	5			-0.3	0.8		313.2		Th(L)
	B	5		10				-0.3	0.8		356.3		P in qtz growth zone Th(L)
	A	8		90				-0.2	0.5		365.7		P in qtz growth zone Th(V)
	C	6		30	5			-0.1	0.3		378.5		P in qtz growth zone Th(V)
	B	4		20				-0.1	0.3		313		P in qtz growth zone Th(L)
	A	8		50				-16.4	18.6				
	A	10		60			-31.9	-17.7	19.5				Double bubble
	A	4		75				-0.3	0.8		384.8		Th(V)
	A	3		75				-0.2	0.5		297		Th(L)
	B	10		20							253.5		Th(L)

901270040b White quartz vein (50 mm) in dark, altered, medium grained quartz diorite.
Abundant, very small (<1-10 micron) secondary inclusions wiht irregular to negative crystal shapes.
Types A, B and D observed. Type A was most abundant with Type B having consistent L/V ratios in individual micro-fractures.

Sample Number	Incl Type	Size microns	Vol % CO2 (L+V)	Vol % H2O vap.	Vol % solids	Tn ice	Te ice	Tm ice	Salinity Wt%CaCl2	Tm CaCl2	Th	Td	Comments
901270040b	B	8		5		-45		-12.4	15.7				
DDH27/215.80	B	10		5		-47	-40	-14.8	18		153.4		Th(L)
	B	15		5		-55	-62	-15.3	18.1				
	B	6		5			-40	-15.4	18.2		97.2		Th(L)
	C	5		5	10			-14.3	17.8		132.8		Th(L)
	B	6		5			-45	-14.4	17.8		185.5		Th(L)
	B	15		5				-13	16.8		123.1		Th(L)
	B	20		5		-58		-3.6	4.5		129.9		Th(L)
	B	10		5		-48	-58	-8.7	12.3		98.6		Th(L)
	B	10		5		-50	-59	-7.2	10.5		93.8		Th(L)

Sample Number	Incl Type	Size microns	Vol % CO2 (L+V)	Vol % H2O vap.	Vol % solids	Tn ice	Te ice	Tm ice	Salinity Wt%CaCl2	Tm CaCl2	Th	Td	Comments
	B	5		5				-15	18		152.9		Th(L)
	B	8		5				-14.2	17.7		134.2		Th(L)
	B	5		5				-13.3	16.9		129		Th(L)

901270045 Vuggy quartz veinlets in sedimentary breccia containing fragments of quartz feldspar porphyry.
Abundant inclusions (<1-20 micron) in quartz.
Primaries observed in quartz cores but most are secondary with irregular to negative crystal shapes.
Types A, B, C (rare) and D are observed. Type A most abundant and Type B have consistent L/V ratios.

Sample Number	Incl Type	Size microns	Vol % CO2 (L+V)	Vol % H2O vap.	Vol % solids	Tn ice	Te ice	Tm ice	Salinity Wt%CaCl2	Tm CaCl2	Th	Td	Comments
901270045	B	10		10				-26.6	33		321.3		P Th(L) growth band on inner qtz core
DDH49/374.60	A	8		40		-75	-60	-26	33.3		461.4		P Th(V) growth band on inner qtz core
	A	6		50				-26.4	33.1		498.4		P Th(V) growth band on inner qtz core
	B	6		10				-25.7	33.4		279.6		P Th(L) growth band on inner qtz core
	B	5		10		-70	-65	-26.6	33		122		P Th(L) growth band on inner qtz core
	A	4		75				-25.6	33.4				
	A	5		70			-55	-26.3	33.1		365.7		P Th(L) growth band on inner qtz core
	A	6		40				-26.8	32.9				
	B	4		5		-70		-33	31.9		321.9		P Th(L) growth band on inner qtz core
	B	5		5			-64	-41.4	30.8		35.9		S Th(L) Outer qtz rim
	B	6		5			-65	-42.6	30.6		76.4		S Th(L) Outer qtz rim
	B	5		5			-63	-39	31.2		80.9		S Th(L) Outer qtz rim
	B	4		5			-65	-42.1	30.5		90.2		S Th(L) Outer qtz rim
	B	4		5			-66	-42.5	30.5		92.6		S Th(L) Outer qtz rim
	B	8		5			-65	-40.4	30.9		75.8		S Th(L) Outer qtz rim
	B	6		5			-63	-48.4	30.1		76.4		S Th(L) Outer qtz rim
	B	3		5		-111		-41.5	30.8		41.7		S Th(L) Outer qtz rim
	B	3		5			-64	-42.3	30.5		68		S Th(L) Outer qtz rim
	B	2		5				-31.2	32.5		109.4		S Th(L) Outer qtz rim
	B	10		10		-75	-67	-31.8	32.1		126.9		S Th(L) Outer qtz rim

901270046 White quartz veinlets and mesh veinlets (from 1 to 10 mm) in dark green, medium grained quartz diorite.
Many, very small (<1-10 micron) secondary inclusions observed.
Types A, B, C and D are observed. however, mostly Types A or D with extensive evidence of necking.
Type C have consistent L/V ratios.

Sample Number	Incl Type	Size microns	Vol % CO2 (L+V)	Vol % H2O vap.	Vol % solids	Tn ice	Te ice	Tm ice	Salinity Wt%CaCl2	Tm CaCl2	Th	Td	Comments
901270046	C	5		5	3			-22.8	23.5		122.5		Th(L)
DDH53/80.90	C	3		5	3		-50	-23.5	22.9		128.9		Th(L)
	C	5		5	3			-23.4	22.9		158.8		Th(L)
	B	8		5				-23	22.7		90.5		Th(L)
	C	4		5	3			-23.3	22.8		85.3		Th(L)
	C	3		5	3			-23.8	22.9		157.9		Th(L)
	C	2		5	3			-22.6	22.4		86.2		Th(L)
	B	5		5				-22.8	22.5		118.3		Th(L)
	B	3		5				-22.6	22.4		121.8		Th(L)

SAMPLES FROM ZONE OF COPPER MINERALISATION

901270062 Massive white quartz
Abundant, very small (<1-20 micron) inclusions with a wispy texture.
Primaries observed in growth bands in vuggy quartz.
Inclusions have irregular to negative crystal shapes with generally inconsistent L/V ratios.
Types A, B, and D are observed.

Sample Number	Incl Type	Size microns	Vol % CO2 (L+V)	Vol % H2O vap.	Vol % solids	Tn ice	Te ice	Tm ice	Salinity Wt%CaCl2	Tm CaCl2	Th	Td	Comments
901270062	A	10		50		-120		-0.7	1.2		331.9		Th(L)
	A	10		35				-0.4	0.7		281.5		Th(L)
	B	10		5			-53	-31.3	25.8		119.2		P Th(L)
	B	10		5		-85	-51	-30.4	25.4		115.9		P Th(L)
	B	8		5				-10	14		141.5		P Th(L)
	B	5		5							142.6		P Th(L)
	B	15		5		-80	-69	-5.6	9.1		74.4		P Th(L)
	A	5		60				-3.1	4.1				
	B	8		10				-5.5	9		240.6		P Th(L)
	B	5		2							65.8		P Th(L)
	B	20		5			-58	-5.2	9		150		P Th(L)
	A	10		40				-4	8.2		340		P Th(L)
	A	10		90							431.1		Th(L)
	B	4		10		-80		-10.8	14.8		249		Th(L)
	B	10		5			-30	-3.5	7		152.8		Th(L)
	B	10		5		-60		-38	-19.6		21		Th(L)
	B	10		5			-51	-34.2	27		110.7		Th(L)
	B	5		10				-3.4	7		239.6		Th(L)

901270064 Quartz vein with hematite.
Abundant inclusions (<1-30 micron) with wispy texture.
Mostly secondary with irregular to rounded shapes and evidence of necking.
Types A, B, C and D observed with Type C having consistent L/V ratios in a single micro-fracture.

Sample Number	Incl Type	Size microns	Vol % CO2 (L+V)	Vol % H2O vap.	Vol % solids	Tn ice	Te ice	Tm ice	Salinity Wt%CaCl2	Tm CaCl2	Th	Td	Comments
901270064	C	10		5	2			-45.8	30.2		78.9		Th(L) 1st micro-fracture
	C	15		5	2	-110	-84	-45.4	30.3		101.3		Th(L) 1st micro-fracture
	C	20		2	1		-80	-45.7	30.2		59.7		Th(L) 1st micro-fracture
	C	8		5	2			-46.1	30.1		84.7		Th(L) 1st micro-fracture
	C	20		5	2		-82	-43.4	30.4		102.7		Th(L) 1st micro-fracture
	C	30		2	2			-45.9	30.2		68.4		Th(L) 1st micro-fracture
	C	30		5	2		-76	-34.1	32		121.7		Th(L) 2nd micro-fracture
	B	5		10							117.4		Th(L) 2nd micro-fracture
	B	10		5							117.5		Th(L) 2nd micro-fracture
	B	10		5				-26.7	24.2		129.2		Th(L) 2nd micro-fracture
	B	10		5			-71	-24.9	23.4		172.2		Th(L) 2nd micro-fracture
	A	5		50			-70	-26.2	24				
	B	15		1			-74	-33.4	26.8		26.3		Th(L) 2nd micro-fracture
	B	15		10		-55	-72	-35.1	27.2		217.7		Th(L) 2nd micro-fracture
	A	8		75		-80		-24.7	23.4		486.2		Th(L) 3rd micro-fracture
	A	5		85				-22.5	22.3				
	B	5		10				-24	22.9		400		Th(L) 3rd micro-fracture
	B	6		5			-63	-36.5	27.5		163.8		Th(L) 3rd micro-fracture
	B	4		10			-63.2	-36.7	27.6		142.2		Th(L) 3rd micro-fracture
	C	10		5	2		-63.5	-33.1	27		374		Th(L) 3rd micro-fracture

901270066 Massive quartz
Abundant small inclusions (<1-20 micron) observed with primaries evident in growth bands.
Inclusions have irregular shapes with evidence of necking.
Types A, B, and D observed. Type B have consistent L/V ratios in individual micro-fractures.

Sample Number	Incl Type	Size microns	Vol % CO2 (L+V)	Vol % H2O vap.	Vol % solids	Tn ice	Te ice	Tm ice	Salinity Wt%CaCl2	Tm CaCl2	Th	Td	Comments
901270066	A	10		80				-29.1	25		411.1		P Th(L)
	B	8		5			-55.2	-25.8	23.6		135.2		P Th(L)
	B	5		5				-30.4	26		95.2		P Th(L)
	A	8		40				-28.8	25				
	B	6		5		-71	-52.1	-25.6	23.4		350		P Th(L)
	C	10		5	2	-80	-53.2	-26.3	24		129.8		P Th(L)
	C	8		5	2	-85	-51.9	-26.1	23.9		117		P Th(L)
	B	10		10		-78	-48.7	-25.3	23.2		128.8		P Th(L)
	B	5		2		-80	-50.2	-26.8	24.3		132.3		P Th(L)
	B	5		2		-79	-51.5	-27.3	24.5		133.4		P Th(L)
	B	8		5		-80	-62.3	-25.7	23.6		128.8		P Th(L)
	B	10		5			-64.7	-27.6	24.7		88.4		P Th(L)
	B	3		10		-80		-32.2	26.8		86.9		P Th(L)
	B	6		5				-23.2	22.6		91.6		P Th(L)
	B	6		5			-50	-16.1	18		92.8		P Th(L)

901270068a Massive quartz.
Abundant inclusions (<1-50 micron) with wispy texture. Large inclusions observed in vuggy quartz.
Secondary, irregular shapes with evidence of necking. Generally inconsistent L/V ratios observed.
Types A, B, C (with up to 3 daughters) and D are observed.

Sample Number	Incl Type	Size microns	Vol % CO2 (L+V)	Vol % H2O vap.	Vol % solids	Tn ice	Te ice	Tm ice	Salinity Wt%CaCl2	Tm CaCl2	Th	Td	Comments
901270068a	A	15		40		-45		-1.9	3.2				
	A	10		35				-1.6	2.7		213.1		PTh(L)
	B	8		5		-40	-34	1.2			168.7		PTh(L)
	B	10		5		-38	-35				142.7		PTh(L)
	B	10		5			-33	-3	5		90.9		PTh(L)
	B	6		5			-35	-2.5	4.2		125.5		PTh(L)
	B	8		5				-2.7	4.5		197.7		PTh(L)
	A	10		35		-44	-44	-3	5				
	C	15		10	5	-46		-4.9	7.8				
	B	8		10		-40		-0.9	1.6		244.5		PTh(L)
	B	5		10		-41		-3.8	6.2		178.1		PTh(L)
													Different micro-fracture
	C	20	10	10		-69	-60	-22.5	22.2		107		Th(L)
	C	20	10	10		-70	-62	-23.9	23.1		121.1		Th(L)
	C	15	5	5		-69	-55	-24.3	23.3		141.5		Th(L)
	C	15	5	1		-68	-56	-22.4	22.3		119.2		Th(L)
	C	10	5	10		-70		-26.3	24.2				
	C	20	5	15		-71	-58				125.3		Th(L)
	C	15	5	2		-50	-63	-24.8	23.8		133.1		Th(L)
	C	15	10	2		-65	-65	-24.8	23.8		124.9		Th(L)
	C	30	10	5		-71	-64	-24.7	23.8		111.1		Th(L)
	D	5				-70	-64	-18.5	20.3				NaCl.2H2O melts at -26.5 C
	B	5	10			-71	-65	-25.4	23.5		114.9		Th(L)
	B	10	5			-72	-66	-25.5	23.5		112.8		Th(L)

901270069 Vuggy quartz veins.
Abundant, irregular to negative crystal shaped inclusions (<1-20 micron) in 2 assemblages.
(i) Primary Types A, B and D in growth zones with inconsistent L/V ratios.
(ii) Secondary Type C inclusions with consistent L/V ratios.

Sample Number	Incl Type	Size microns	Vol % CO2 (L+V)	Vol % H2O vap.	Vol % solids	Tn ice	Te ice	Tm ice	Salinity Wt%CaCl2	Tm CaCl2	Th	Td	Comments
901270069	C	10		5	2			-19.3	20.9		101.1		P Th(L)
	C	5		5	5	-54	-46	-19	20.7		122.5		P Th(L)
	B	4		5				-22	22.2		103.4		P Th(L)
	C	20		5	2	-75	-62	-21.5	21.9		110.6		P Th(L)
	C	10		5	2		-54	-18.8	20.3		89.7		P Th(L)
	C	6		5	5	-61	-55	-21.5	21.9		103.7		P Th(L)
	C	10		5	2	-60	-52	-20.1	21.5		104.4		P Th(L)
	B	10		5			-55	-20.9	20.7				
	C	20		5	2	-62	-67	-22.4	22.3		106.3		P Th(L)
	C	10		5	2			-22	22.2		99.3		P Th(L)
	C	10		5	2			-22.7	22.5		184.3		P Th(L)
	B	5		10		-50	-53	-19.3	20.9				
	B	15		5				-20.7	21.6		154.5		P Th(L)
	B	3		10			-51	-18.5	20.2		131.2		P Th(L)
	B	5		5				-19	20.7		155.1		P Th(L)
	B	5		5			-50	-18.5	20.2		156.2		P Th(L)
	B	6		5			-54	-21.7	22		224		P Th(L)
	B	15		10			-52	-21.3	21.7		217.6		P Th(L)
	B	8		10			-54	-18.9	20.7		169.2		P Th(L)
	C	8		5	2	-76		-20.6	21.5		262.5		P Th(L)
	B	5		5			-56	-21.7	22		133.4		P Th(L)
	B	4		5		-60	-56	-31.4	26		133.5		P Th(L)
	B	5		5			-55	-31.6	26.1		165.8		P Th(L)